PARAMETRIC AND PERFORMANCE ANALYSIS OF A HYBRID PULSE DETONATION/TURBOFAN ENGINE

By

SIVARAI AMITH KUMAR

Presented to the Faculty of the Graduate School of

The University of Texas at Arlington in Partial Fulfillment

Of the Requirements

For the Degree of

MASTER OF SCIENCE IN AEROSPACE ENGINEERING

THE UNIVERSITY OF TEXAS AT ARLINGTON

May 2011

ACKNOWLEDGEMENTS

This thesis would not have been possible without the guidance and help of all my supervisors, professors, lab mates, family and friends. I would like to thank Dr. Wilson who guided me throughout the project, without whom this thesis would not have been possible. I would like to extend my gratitude to Dr. Frank Lu to make me a part of the Aerodynamics Research Center (ARC) and for all the support he has been giving me in all the lab meetings. I would like to thank Dr. Frank Lu and Dr. Haji-Sheikh for agreeing to be on the defense committee, and reviewing my thesis. I would also like to thank Eric Brawn and Kishore Nekkanti for giving me suggestions and helping me in proceeding with my thesis.

My inspiration and strength throughout my masters is my best friend Sneha Ganesh Iyer, without whom staying in UTA would not have been possible. I owe a lot to my well-wishers Ganesh Iyer, Lalitha Iyer and Praneeth Kotapalli.

Finally, I would like to thank my family for their unwavering and continued support and encouragement throughout my education. I would also like to thank my friends who have always been supportive throughout my stay in UTA.

April 29, 2011

ABSTRACT

PARAMETRIC AND PERFORMANCE ANALYSIS OF A HYBRID PULSE DETONATION / TURBOFAN ENGINE

SIVARAI AMITH KUMAR, M.S

The University of Texas at Arlington, 2011

Supervising Professor: Donald Wilson

The performance of a hybrid pulse detonation engine (PDE), with the PDE tubes installed in the bypass duct of a turbofan engine is investigated in this study. Performance parameters for the duct burning PDE engine are compared with a baseline turbofan engine. The PDE analysis is based on an updated numerical analysis by Endo-Fujiwara, whereas the turbofan calculations are based on Mattingly's gas turbine model. The calculations were done with MATLAB 2010 as a platform. A mixer analysis was performed for the hybrid engine concept. In the duct burning PDE, the PDE exhaust was mixed with the turbine exhaust prior to entering the nozzle. For this configuration, core air was mixed with the PDE exhaust to cool the flow prior to entering the turbine. The performance of both configurations was compared for parametric variations of compressor and fan pressure ratio, bypass ratio, PDE tube length and frequency. A performance analysis was carried out for the resulting hybrid baseline engine at different altitudes and Mach numbers.

TABLE OF CONTENTS

LIST OF ILLUSTRATIONS

LIST OF TABLES

CHAPTER 1

INTRODUCTION

Research on pulse detonation engines (PDE) has increased dramatically over the past decade due to high theoretical performance. Advantages of having a PDE as the propulsion device, such as lower cost and simplicity compared to conventional gas turbines, provided the motivation for its development. For more than half a century, experiments have been carried out exploring the use of detonation for propulsion applications [1]. Experiments on PDE involving rapid mixing of the fuel and air at high speeds have been carried out, which predicted improved performance compared to Gas turbine engines.

The PDE provides the potential for major advancements in modern propulsion technology. The PDE generates thrust with repetitive cycles of detonation, wave propagation through the detonation chamber and thrust expulsion out of it. Therefore, the process involves initiating and sustaining a detonation in a controlled manner. The total pressure exiting the tube must be exploited to create maximum thrust. There are at least two applications of PDE that can be related to a gas turbine engine. The first application is replacing the main combustor with a PDE combustor. In this configuration the PDE exhaust drives the downstream turbine which provides power to compressor. The second application is introducing PDE tubes in the bypass duct of a turbofan, in which the PDE exhaust is mixed with the core flow for thrust generation. Integration of the PDE into a gas turbine engine requires understanding of the underlying physics of the PDE. Because of the simple geometry of the PDE, Computational Fluid Dynamics (CFD) methods can be used to estimate the performance and can provide detailed prediction of the flow structure, but classical analytical methods can be used to complement experiments and are useful in understanding basic physical phenomena as well as providing a

useful tool for performing parametric design studies of PDE. Here we adopt a numerical analysis of the PDE provided by Endo-Fujiwara [29-31] to predict the performance of the basic PDE, and the performance of a hybrid PDE/turbofan engine.

The turbofan has its maximum efficiency at subsonic speed rather than supersonic speeds. Pulse detonation engines are much more efficient in the process of combustion when compared to the turbofan engines. This process involves a detonation wave which compresses and burns the fuel/oxidizer mixture and in return results in high pressures and temperature. Deflagration to Detonation Transition (DDT) is used in PDE for initiating the combustion process compared to deflagration technology in commercial turbo machinery.

The PDE can theoretically operate with greater thermodynamic efficiency than the comparable constant pressure combustion process of conventional gas turbines. Application of PDEs range from stand-alone propulsion systems, in combination with a conventional propulsion system, or as a hybrid turbofan or turbojet engine, where the conventional combustion chamber is replaced by the PDE combustion chamber or PDE tubes are installed in the bypass ducts surrounding the gas turbine core.

1.1 Pulse Detonation Engine (PDE)

PDE engine operates in a pulsating mode, and a very aggressive energy conversion rate occurs through the detonation process and in-turn is the key feature of such an engine. Because of the rapid series of events, fuel is burned as a self-sustaining detonation wave propagating through the combustion chamber and this overall process is thermodynamically closer to a isochoric (constant volume) process rather than the isobaric (constant pressure) process typical of conventional propulsion systems. This implies that greater cycle efficiency can be expected. Cycle time is the only limitation for the performance of the engine. Although the PDE has an edge over conventional gas turbines, it has its limits such as sound level during

the detonation process, which is more than human audible range (Allgood [50]) and open end cracking after a long period of operation, due to thermal fatigue (Schauer [42]).

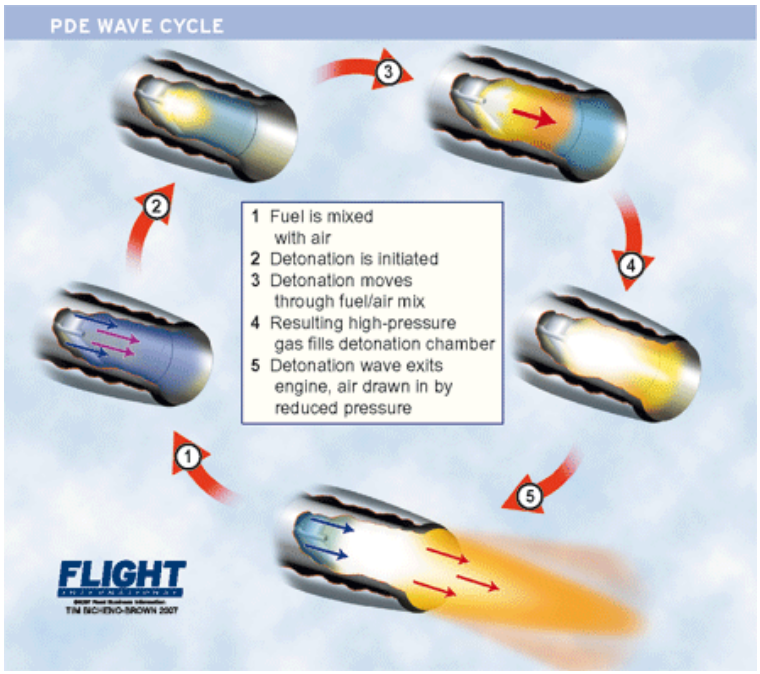

Fig 1.1: PDE wave cycle (Ref[49])

1.2 Detonation and Mixing

Detonation is a form of combustion that differs significantly from deflagration. The process of burning fuel rapidly with a flame front that travels at subsonic speed defines deflagration, and is the type of combustion found in conventional gas turbine engines and rockets. However, detonation is a violent reaction that travels at supersonic speeds relative to the unburned reactants, and produces an increase in pressure, compared to the pressure drop that occurs in deflagration burning. The overall process is thermodynamically closer to a

constant volume process, and it is more efficient than the constant pressure process used in conventional gas turbines (deflagration).

The rapid initiation of a detonation is a challenging aspect of PDE research. Direct initiation and deflagration-to-detonation transition (DDT) are two methods to initiate detonation, but direct initiation requires large energy expenditure. DDT is slow and a highly detonable mixture is needed for this process to overcome this limitation pre-detonators have been used (Tegner [25]). Bussing and Pappas [27] provide a good explanation of detonation methods and the DDT process.

1.3 Simplicity, Efficiency and Limits

A PDE, when compared to conventional deflagration engines, has many advantages. First of all, it has almost no moving parts except the valves, giving a high thrust to weight ratio. Second, the simple design of the PDE requires less volume, giving another reason for integration of the PDE with turbo machinery. Thrust is directly proportional to frequency (Mawid [41]) and the thrust is produced more efficiently, which is shown by studies of Heiser and Pratt [4] and Edelman and Yang (1998). Lastly, the thermodynamic efficiency of the PDE cycle results in a higher theoretical performance across all flight envelopes and has the potential advantage of increased thrust and lower TSFC compared to normal propulsion systems.

Simple design of the PDE has many advantages compared to other propulsion systems. Simple maintenance because the lower part count compared to other propulsion systems, makes it lighter than others, with better thrust to weight ratio. The major advantage of the PDE is its design which works on simple mechanical principles. Jet engines need fuel injection pumps to inject high pressure fuel for thrust generation, whereas the PDE cycle process itself creates high pressures within the PDE tube, which is needed for maximum thrust generation.

For every positive feature of PDE, there are negatives as well. One negative feature is the hammer shock near the inlet of a PDE resulting in near choking and damaging the valve. Another negative feature is the sound level which is more than the human audible level (Allgood [51]).

1.4 Hybrid Pulse Detonation Engine/Turbofan

A hybrid pulse detonation engine (PDE) using duct burning would combine the PDE combustor in the bypass duct of a conventional mixed-flow turbofan. The core engine stays unaffected but the bypass air would flow into a bank of PDE tubes. This combination would yield significantly more thrust requiring additional fuel.

The hybrid PDE is a relatively new concept topic to be investigated. Hybrid engines are of two types, one in which the PDE replaces the conventional combustor, but has the disadvantage of providing high temperature flow into turbine blades. An alternate approach involves arranging the PDE combustor in the bypass duct and mixing the PDE exhaust with the turbine exhaust in a mixer located aft of the turbine. The following sections discuss the physics of detonation, PDE and the Hybrid PDE/TF concept.

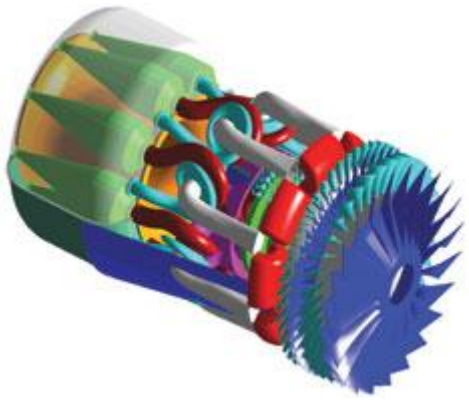

Fig 1.2: A concept for a hybrid engine combines conventional turbo machinery principles with a pulse detonation engine[50]

1.5 Objective and Approach of Current Research

The objective of this study is to demonstrate the potential performance gain of a hybrid pulse detonation/turbofan using PDE tubes placed in the bypass duct of a turbofan engine. The study incorporates a mathematical model of the PDE based on an updated model by Endo and Fujiwara [29, 30, and 31] to study the variation of PDE performance resulting from different lengths and frequencies. The next step is to generate a mathematical model the integration of high thrust producing PDE tubes with a conventional turbofan. The turbofan analysis is based on Mattingly's gas turbine design model [34]. A parametric cycle analysis on the hybrid PDE/turbofan engine is conducted to show the trends of specific thrust and specific fuel consumption. The effects of different fuel mixture compositions, altitude and Mach number variation was investigated to provide a better understanding of the performance of the hybrid engine. A mixer is required to reduce the PDE exhaust temperature prior to the flow passing the turbine blades. The goal of this study was to investigate the effects of incorporating the PDE in the bypass duct on specific thrust and TSFC.

CHAPTER 2

LITERATURE REVIEW

Pulsed detonations have been explored extensively for propulsion applications because of their inherent theoretical advantage over deflagrative combustion [16]. The work done by GE global research [4-15] and NASA [1, 13] suggest that of integrating pulsed detonation with turbo machinery would result in a more efficient engine with mechanical simplicity. Paxson [13] used CFD cycle results to calculate pulse detonation combustor performance, where the pulse detonation replaced the normal combustion chamber in a turbofan or turbojet. This method was used by GE Global Research to achieve a converged pulse detonation cycle which described cycle time of the process. Paxson's work with minor modification was selected for PDC work as it showed the ability to base a performance map on experimental data. A parametric study presented by Tangirala et al [17] stated that assuming constant specific heat through a PDC analysis resulted in prediction of total pressure ratios and cycle time, but with flaws.

Kailasnath [16] discussed different types of detonations such as pulse detonations and rotating detonations. His revision predicted an increase in efficiency through detonations when compared to a constant pressure or constant volume process. One of the observations of the report was an increase in the efficiency by introducing a nozzle and its effect on detonation transmission. The observation from experimental studies by Schauer et al. [42] yielded the effects of equivalence ratio on thrust, impulse and specific fuel consumption. Impulse was found to decrease with increasing equivalence ratio. Schauer et al [42] also noted that when the detonation was vented into a turbine, the blow down times of a single PDE tube

increased, extending the fill portion for next cycle. In the numerical simulation by He and Kadagozian [36], a one-step reaction model for hydrogen-air and methane–air was suggested. Their results predicted the noise levels by measuring pressure history at different locations and concluded that the calculated impulse is not dependent on geometry. Experimental studies were carried out by Schauer et al, [43] with a coupled PDE/ turbocharger to investigate the power extraction via mechanical shaft, and they observed a reduction in wave speed at the exit of the turbofan and an increase in the blow down time when the PDE was exhausted into the turbine, which raised the back pressure on the PDE tube. The main observation of the study was that even after 50,000 detonations the turbine was not affected structurally. The experimental and numerical studies on PDE by Rasheed et al, [9] validated the observation of upstream reflection of the shock wave from the turbine blades, as reported in Schauer et al, [43]. Single and multi-cycle analyses were carried out through CFD and experimental studies, but both were never compared. Schauer et al, [43] and Rasheed et al,[9] observed the pressure, temperature and mass flow rate at different locations and stated that multi cycle analysis has to be considered when PDE interaction with turbo machinery was studied. Thermodynamic performance predictions for PDE done by Dyer and Kaemming [5], when compared with ramjet performance, showed less entropy at the exit and higher energy for the former. Their work resembles the PDE cycle proposed by Heiser and Pratt but differed in the calculation of detonation tube exit properties. CJ entropy coupled with the system enthalpy was proposed as an accurate representation of available energy. But the drawback of using the method of Heiser and Pratt [4] is that it neglects the fill portion, and energy is not conserved in this method. Therefore they are unable to predict the time averaged values of the properties.

One of the challenges of integrating a pulse detonation combustor (PDC) into hybrid engine is to predict the interaction between the cyclic detonations and the flow through the turbines. Andrus [47] conducted a numerical analysis of a PDC, replacing the regular combustion chamber and predicted an 8% decrease in fuel consumption while maintaining the

thrust. He stated that to maintain efficiency of the baseline engine, a pulsed engine will require power extraction from the exhaust fluid. A series of tests was carried out on an eight tube PDC exhausted into turbines by GE Global Research [17-19], providing insight into how a PDC interacts with a turbine. And GE has performed several CFD and experimental studies on pulse detonation effects on flow through a turbine which investigated the interaction of the waves with a 2D stator blade. Their results were significant as they showed pressure and temperature rise and fluctuation of mass flow across the turbine, which affects the rotor stages by the enormous stress created.

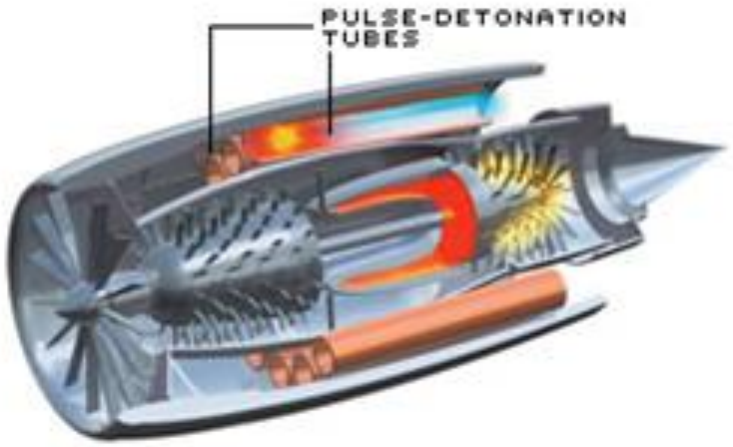

Fig 2.1: PDE tubes in the bypass of a turbofan engine [51]

2.1 Thermodynamic model

The PDE is often modeled as constant volume process or Humphrey cycle, rather than constant pressure process or Brayton cycle, which is the basis of conventional propulsion systems. In the Humphrey cycle, the constant pressure process is replaced by constant volume combustion process. The Humphrey cycle is a cycle that has been used as a surrogate for the pulse detonation cycle to predict performance.

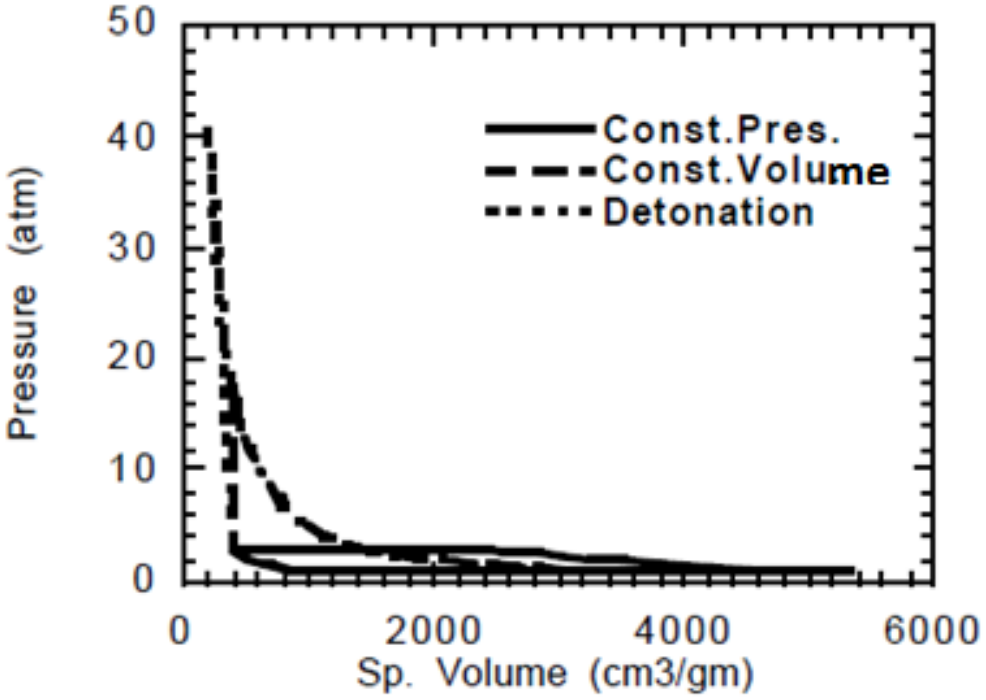

Fig 2.2 Comparison of idealized thermodynamic cycles for constant pressure, constant volume and detonation modes of combustion [15].

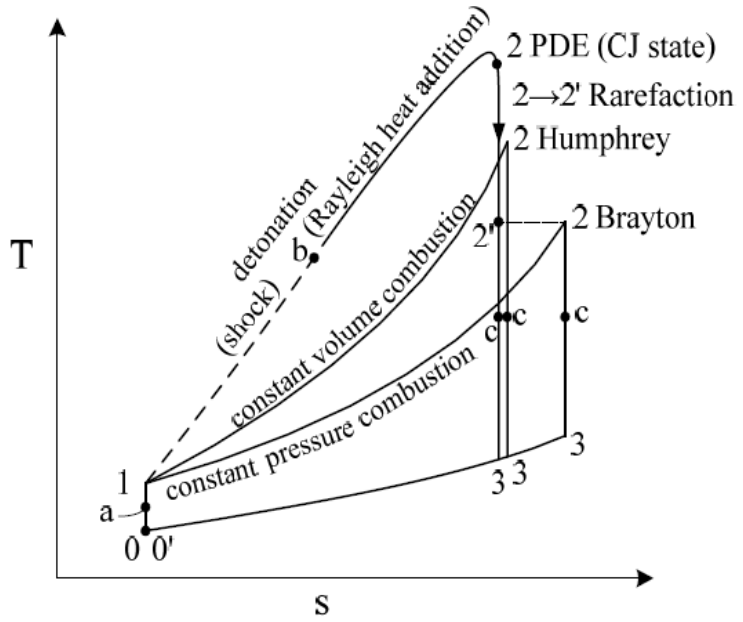

Fig 2.3: Ideal cycle analysis [T-S Diagram] for the Brayton, Humphrey and PDE processes [19].

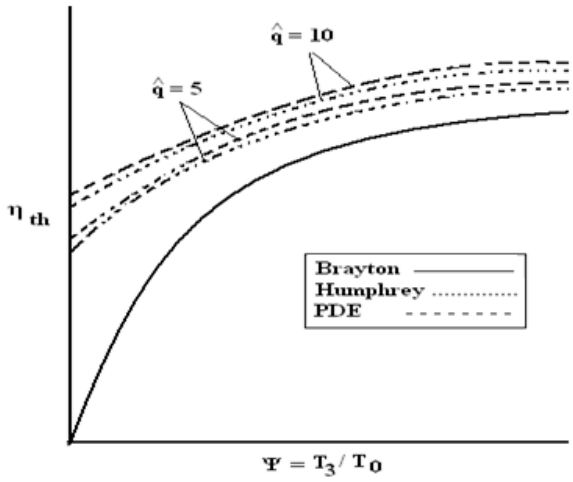

Fig 2.4: Thermal efficiency of Brayton Humphrey and PDE cycles

The efficiency of the Brayton and Humphrey cycle is formulated as

For Brayton cycle,

$$\eta_{th} = 1-(T_o/T_3)$$

For Humphrey cycle

$$\eta_{th} = 1 - (1/\hat{q})\left[(1 + \gamma\hat{q}/\varphi)^{1/\gamma} - 1\right]$$

Where $q = f^{*}h_{PR} / C_pT_o$ and $\varphi = T_3/T_o$.

The thermal efficiency of the Humphrey cycle is less than that of the PDE cycle as the PDE cycle efficiency is given by

$$\eta_{th} = 1 - \left[\frac{1}{M_{CJ}^{\ 2}}\left(\frac{1 + \gamma M_{CJ}^{\ 2}}{\gamma + 1}\right)^{\frac{(\gamma+1)}{\gamma}} - 1\right]\Big/\hat{q}$$

The cycle analysis of Heiser and Pratt employs a generic non-dimensional heat release parameter q, which is the function of equivalence ratio a lower heating value of the fuel air mixture. This heat release parameter was used to calculate the relative performance of the PDE, Humphrey and Brayton cycles [19].

Equivalent q values were used for the all three cycles, assuming all of the ideal engines operated with the same initial conditions and the same amount of heat added during the cycles. A result of their analysis is shown on a temperature-entropy plot, Fig 2.3.The corresponding thermal efficiency curves are shown in Fig. 2.4 and for selected parameters the Humphrey cycle closely simulates the PDE cycle. However it was shown that with non-isentropic component efficiencies, the Humphrey cycle remains high, whereas the PDE cycle falls off significantly. Heiser and Pratt [4] stated that the pulsed detonation engine cycle is

similar to the ideal Humphrey cycle, with the exception of the heat addition during the combustion process. Fig. 2.5 shows the compression process [0-1] for three cycles. The isochoric assumption yields an underestimate of efficiency because the ideal efficiency of detonation cycle is the highest followed by Humphrey and Brayton cycle [19]. Fig. 2.4 shows that the thermal efficiency of PDE cycle is slighter greater than that of the Humphrey cycle and much greater than the Brayton cycle.

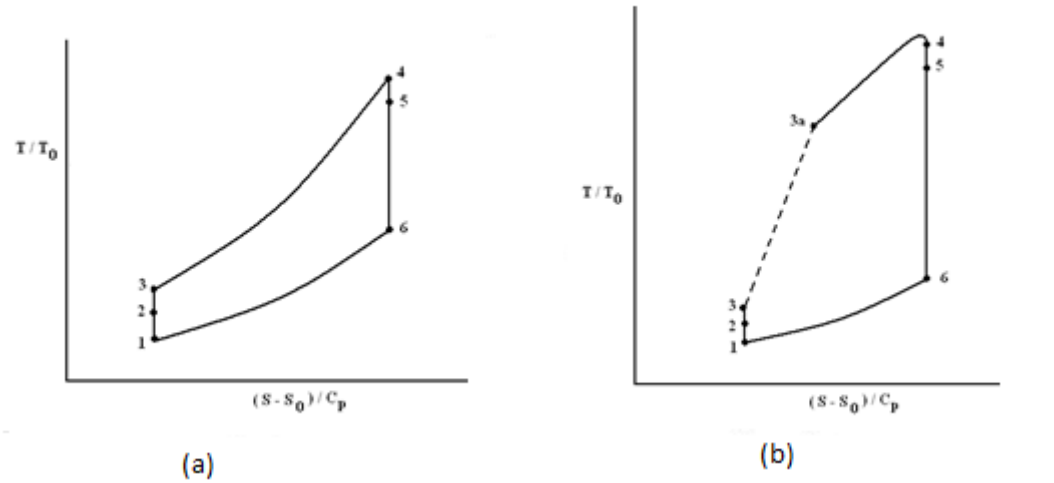

Fig 2.5: T-S diagram for (a) Brayton cycle, (b) PDE cycle [4]

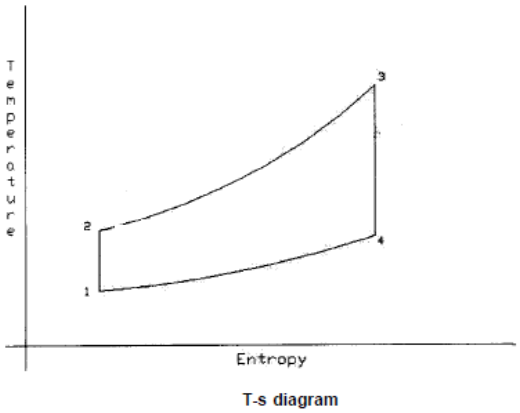

Fig 2.6: T-S diagram of Humphrey cycle [4]

The amount of heat added is the same for the three cycles; the mode of heat addition is the only difference in the three cycles. Heat is added at constant pressure in the Brayton cycle, constant volume for the Humphrey cycle, and by detonation for PDE cycle. Fig. 2.5 shows the process as heat is added at constant pressure as step (2-5) shown in the Fig. 2.5 (a) and step (2-3) in Fig. 2.5 (b) by constant volume combustion. Detonation results in a lower entropy rise and more work when compared to the Brayton cycle. The PDE cycle includes four processes: Isentropic compression, constant volume combustion, isentropic expansion, isobaric heat rejection.

The Humphrey cycle in comparison with the Brayton cycle is shown in the Fig 2.7

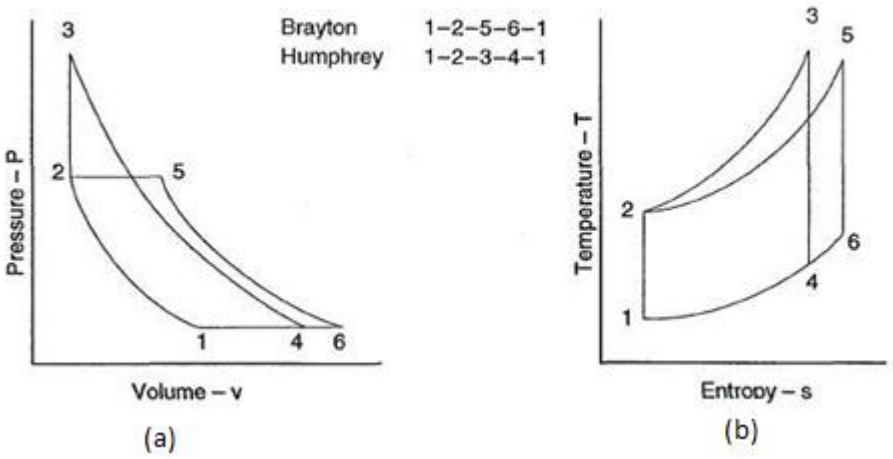

Fig 2.7 Pressure–Volume and Temperature-Entropy diagram for
(a) Brayton cycle, (b) Humphrey cycle.

2.2 Theory of Detonation Waves

The fundamental concept of operation of the PDE is based on detonation combustion. Detonation is defined as a shock wave propagating at supersonic velocities into unburned gas

that is sustained by the energy released by the combustion process [16]. The chemical process during detonation releases energy which drives the wave towards the exit.

A simplified analysis is performed on the detonation wave because of its structure, which is very complex and three dimensional with transverse wave segments as shown in Fig. 2.8[7]

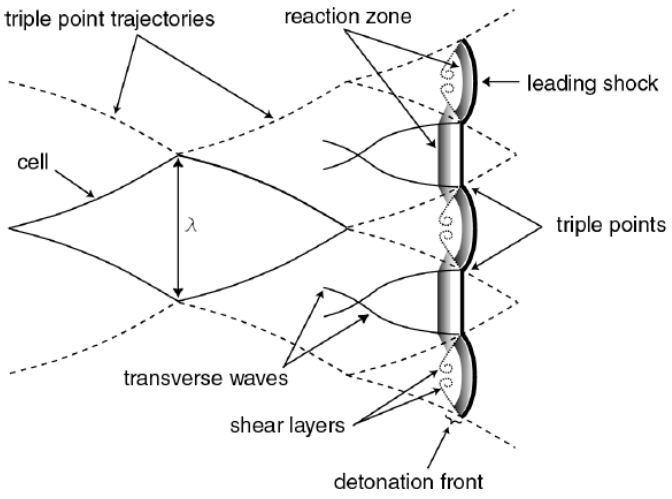

Fig 2.8: Detonation Structure [7]

The Chapmen-Jouguet (CJ) theory and ZND (Zeldovich, von Neumann and Doering) theories are two of the simplified theories for the detonation structure.

2.2.1 Chapman-Jouguet (CJ) Theory

Thermodynamic analysis relating the flow upstream of the combustion wave to the flow conditions downstream of the wave is demonstrated by Chapman-Jouguet theory. The assumptions made for this theory are

- One-dimensional flow
- Ideal gas behavior
- Constant and equal specific heats

- Adiabatic conditions.

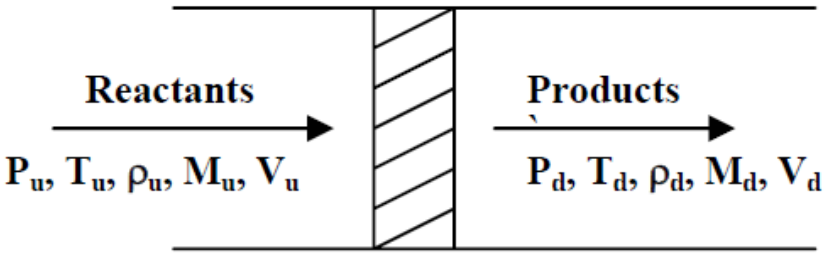

Fig 2.9: Control volume used in the Chapman-Jouguet theory

And applying the continuity, momentum and energy equations to the control volume, gives the following equations

$$\rho_u v_u = \rho_d v_d \quad (3)$$

$$p_u + \rho_u v_u^2 = p_d + \rho_d v_d^2 \quad (4)$$

$$h_u + \frac{v_u^2}{2} = h_d + \frac{v_d^2}{2} \quad (5)$$

The Rayleigh-Hugoniot relation can be obtained from simultaneous solution of the continuity and momentum equations (3) and (4), and the relation of initial state to the final state, and is given by [16].

$$p_d - p_u = -m^2\left(\frac{1}{\rho_d} - \frac{1}{\rho_u}\right) \qquad (6)$$

The Rankine-Hugoniot relationship is obtained by conservation of mass and momentum in addition to conservation of energy which is given by

$$h_d - h_u = -\frac{1}{2}\left(\frac{1}{\rho_d} - \frac{1}{\rho_u}\right)(p_d - p_u) \qquad (7)$$

Thermodynamic properties across the discontinuity and locus of the possible solution for downstream properties can be predicted by the above equation. And the Hugoniot curve is shown below.

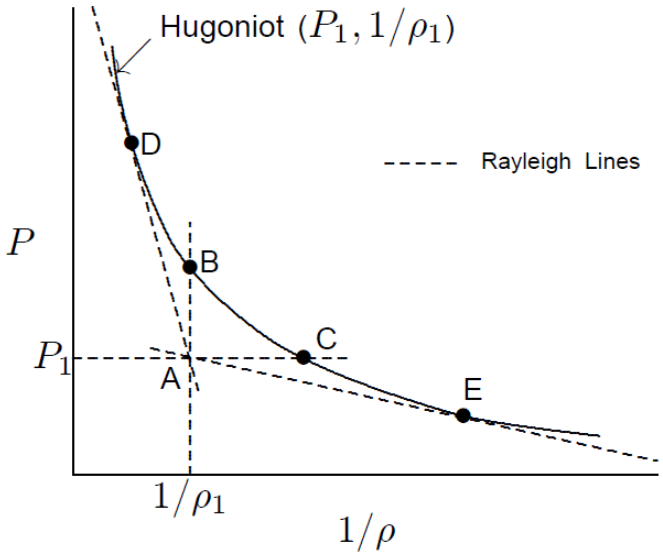

Fig 2.10: Hugoniot Curve [17]

The points where the Hugoniot curve and Rayleigh lines are tangential to each other are called CJ points [16].The Upper CJ (U) and lower CJ (L) corresponds to the detonation and deflagration modes of combustion.

In the Hugoniot curve, there are five regions and the physical phenomena of those regions are given below

- Region A is for strong detonation and subsonic burned gas velocity (deflagration) respectively.
- Region B is for weak detonation and supersonic burned gas velocity.
- Region C, where Hugoniot and Rayleigh conditions are not satisfied, does not represent real solutions. No Rayleigh line can be drawn between regions B and D.
- Region D is for weak deflagration and subsonic burned gas velocity.
- Region E is for strong deflagration and supersonic burned gas velocity

The lower CJ point represents the separation of the strong and the weak deflagration region. The speed at that point is the CJ deflagration velocity. The upper CJ point represents the separation of the strong and the weak detonation region [18]. Minimum entropy exists at the upper CJ point and maximum entropy at lower CJ point. Velocity of the detonation wave is the main outcome of this theory.

2.2.2 ZND Theory

The ZND (Zeldovich (1940), von Neumann (1942), and Doering (1943) theory is also a one-dimensional analysis of a detonation wave. The reactions that occur behind the shock wave in the detonation structure are not considered in CJ theory. The originators of the ZND theory proposed that a detonation wave can be modeled as a strong shock wave coupled with a reaction zone [16].

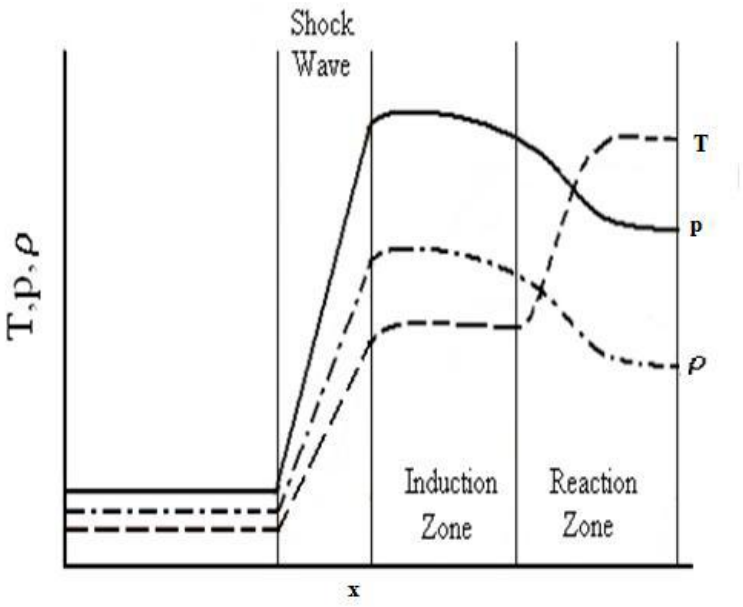

Fig 2.11: Variation of physical properties through a ZND detonation wave [17]

The maximum pressure and temperature corresponds to the von Neumann state. Temperature, pressure, density and area nearly constant immediately behind the shock wave. This region just after the shock is termed as the induction zone. After the induction period, the chemical reaction rates increase, resulting in an increase in temperature, while pressure and density decreases due to expansion of the burned products. The zone where the properties come to an equilibrium (C-J) state is termed the reaction zone. Detailed chemical mechanisms can be used to capture the chemistry occurring in the reaction zone. The expansion wave produced between the end of the reaction zone and upstream boundary wall of the chamber is known as the Taylor rarefaction wave.

CHAPTER 3

CYCLE ANALYSIS OF A PDE

A PDE is a tube with one closed end and the other end open that is filled with a combustible mixture that is ignited at the closed end, creating a detonation wave that travels towards the open end and exits out of the tube.

The cycle procedure demonstrated in Endo and Fujiwara [29, 30, and 31] is illustrated in Fig. 3.1 and each step is discussed below.

- As the rotary valve is opened the tube is filled with fuel/oxidizer mixture and the valve is closed.
- The fuel/oxidizer mixture is then ignited at the closed end therefore resulting in the initiation of a detonation wave.
- The (CJ detonation wave) propagates through the tube, followed by a rarefaction wave known as the Taylor rarefaction wave.
- The detonation wave exits the tube and expands into the atmosphere. The tube is filled with residual burned gases at pressure and temperature levels higher than ambient conditions.
- As the burned gases exit the tube, an expansion wave is propagated from the open end of the tube towards the closed end. This results in lowering the pressure resulting in the expulsion of combustion products from the tube (blow down process).
- The expansion waves, after being reflected off the closed end (thrust wall), exit the tube, further lowering the pressure and the burned gases are exhausted.

- As the combustion products are expelled from of the tube, purge air is used to expel the remaining combustible products followed by subsequent refill of the detonation tube with a fresh fuel/oxidizer mixture, starting a new cycle.

The entire cycle repeats at a frequency on the order of 100 Hz, resulting in a periodic high-pressure zone near the closed end of the chamber. The integrated effect of this high pressure over the closed end (thrust wall) produces thrust. The detonation/blow down process occur when the valve is closed and the purging and filling processes occur when the valve is open. The total time of the cycle can be summarized as

T = Tplateau + Texhaust + Tpurge

The purging of the burned gases is necessary to avoid pre-ignition of the fresh mixture before detonation initiation.

The events in one cycle are shown schematically in Fig 3.1.

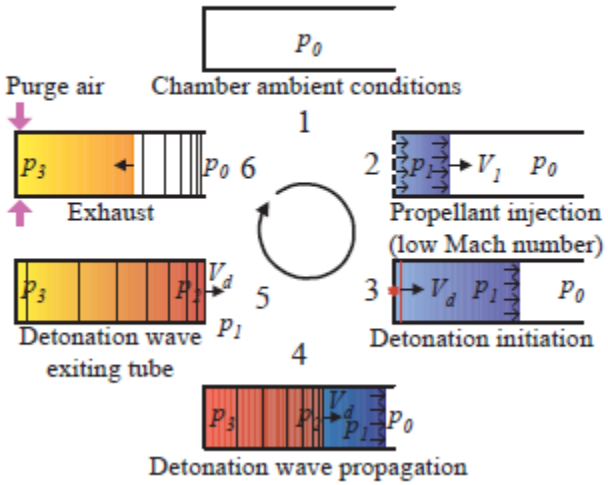

Fig 3.1: Cycle process in ideal pulse detonation engine [53]

After the detonation process, an expansion wave is reflected towards the closed end. This interacts with the Taylor rarefaction wave propagating from closed to open end and

accelerates the fluid towards the open end, thus decreasing pressure at closed end. At the end of the blow down process, the pressure falls below ambient. In a PDE, the closed end propagates an expansion wave through the tube to decelerate the filling process, while the expansion wave is dominated by detonation as soon as it is initiated from the closed end. The specific thrust and TSFC depends upon the initiation of the detonation wave, the blow down period and the purge and refilling period.

When purging ends, the filling process takes place immediately. Injection of the fuel-air mixture is controlled by a valve which separates high-pressure air that was compressed through the fan and burned gases at ambient pressure and elevated temperature. Opening it causes the pressurized air to expand into the detonation tube, therefore resulting in a shock wave. This shock wave propagates into the detonation tube expelling the burned gases. The fuel-air mixture is injected after purging which prevents pre-ignition of the fuel air mixture.

Endo and Fujiwara proposed analytical models [29, 30] where no empirical parameters were included and the model was usable only for qualitative prediction of PDE performance because the rarefaction wave through which the burned gases were exhausted was not correctly treated [32]. The following analysis is formulated with no empirical parameters to predict the pressure history at the thrust wall of a simplified PDE.

An Important contribution of the current work is the formulation of the decay portion of the pressure history at the thrust wall. Prediction of the time at which overpressure at the thrust wall turns negative can be calculated, which is a key parameter, when determining the time sequence of the valves of a PDE.

3.1 Analytical Model of PDE

The pulse detonation engine (PDE) is modeled as a straight cylindrical tube with fixed cross section with one end closed and other open as shown in the Fig 3.2. One-dimensional flow of a calorically perfect gas is considered without viscous effects and thermal conduction.

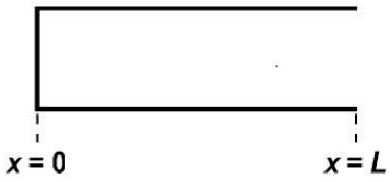

Fig 3.2: PDE tube

The gas dynamics and formulation of local gas properties, cycle time (Tcyc), frequency (f) and Impulse (I) are presented below.

The cycle starts when the undisturbed gas, which is characterized by γ_1, P_1, a_1, and u_1 $(=0)$ at the time t =0 at position x=0, is ignited resulting in the initiation of a detonation wave (CJ wave) which propagates towards the open end. The front of the detonation wave is the von Neumann spike behind which chemical reaction occurs. The burned gas due to the reaction at the rear surface of the detonation wave is characterized by γ_2, P_2, a_2, and u_2. Time t_1 is when the CJ wave reaches the exit of the detonation tube.

The parameters (P_2, a_2, and u_2) of the burned gas at the rear of the detonation wave are given by following equations based on the model by Endo and Fujiwara [32].

$$p_2 = \frac{\gamma_1 M_{CJ}^2 + 1}{\gamma_2 + 1} p_1 \quad (3.1)$$

$$a_2 = \frac{\gamma_1 M_{CJ}^2 + 1}{\gamma_1 M_{CJ}^2} \frac{\gamma_2}{\gamma_2 + 1} D_{CJ} \quad (3.2)$$

$$u_2 = \frac{\gamma_1 M_{CJ}^2 - \gamma_2}{\gamma_1 M_{CJ}^2} \frac{1}{\gamma_2 + 1} D_{CJ} \quad (3.3)$$

X_2 is defined the position of the rear surface of the detonation wave and it is given by

$$x_2 = D_{CJ} t \quad (3.4)$$

The time when the detonation wave reaches the closed end can be written as

$$t_{CJ} = L / D_{CJ} \quad (3.5)$$

where D_{CJ}= Detonation wave speed and L = length of the tube

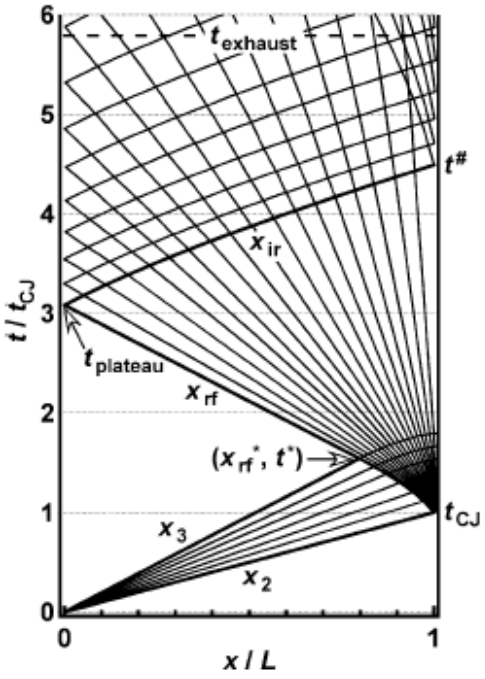

Fig 3.3: Space–ttime (*x*–*t*) diagram of characteristics in a simplified PDE [31].

The flow is decelerated to U3=0 via a rarefaction wave following the detonation wave known as the Taylor rarefaction wave. The rear surface of the CJ wave is coincident with the front boundary of the Taylor rarefaction wave.

The relation of the gas properties inside the Taylor wave, represented by the region $X_3<X< X_2$, is given by [31]

$$p = \left(1 - \frac{\gamma_2 - 1}{\gamma_2 + 1}\frac{x_2 - x}{a_2 t}\right)^{2\gamma_2/(\gamma_2 - 1)} \frac{\gamma_1 M_{CJ}^2 + 1}{\gamma_2 + 1} p_1 \qquad (3.6)$$

$$a = \frac{\gamma_1 M_{CJ}^2 + \gamma_2}{\gamma_1 M_{CJ}^2}\frac{1}{\gamma_2 + 1} D_{CJ} + \frac{\gamma_2 - 1}{\gamma_2 + 1}\frac{x}{t} \qquad (3.7)$$

$$u = -\frac{\gamma_1 M_{CJ}^2 + \gamma_2}{\gamma_1 M_{CJ}^2}\frac{1}{\gamma_2 + 1}D_{CJ} + \frac{2}{\gamma_2 + 1}\frac{x}{t}(<a) \qquad (3.8)$$

where M_{CJ} = Detonation Mach number.

The parameters ($p3$, $a3$, and $x3$) of the gas on the rear surface of the decelerating rarefaction wave (Taylor wave), which is the same for the region 0<x< X3 are given by

$$p_3 = \delta_{A1} p_1 \qquad (3.9)$$

$$a_3 = D_{CJ}/\delta_{A2} \qquad (3.10)$$

$$x_3 = a_3 t \qquad (3.11)$$

where

$$\delta_{A1} = \frac{\gamma_1 M_{CJ}^2 + \gamma_2}{2\gamma_2}\left(\frac{\gamma_1 M_{CJ}^2 + \gamma_2}{\gamma_1 M_{CJ}^2 + 1}\frac{\gamma_2 + 1}{2\gamma_2}\right)^{(\gamma_2 + 1)/(\gamma_2 - 1)} \qquad (3.12)$$

$$\delta_{A2} = 2\frac{\gamma_1 M_{CJ}^2}{\gamma_1 M_{CJ}^2 + \gamma_2} \qquad (3.13)$$

The end wall pressure (p_3) is the plateau pressure in the thrust history and one of the important parameter characterizing performance of a PDE [31]. The position of the rear boundary of the decelerating rarefaction wave is given by X_3. As the detonation wave exits from the open end of the tube, another rarefaction wave is generated which propagates from the open end towards the closed end of the tube, starting at t_{CJ}. This rarefaction wave exhausts the burned gas from the open end of the tube. The front boundary of the reflected rarefaction wave initially propagates in to the decelerating rarefaction wave and intersects the rear boundary of

the decelerating Taylor rarefaction wave at the time t^* and at location X_{rf}^* and propagates towards the closed end of the tube [31]. The critical time and location relations are given by

$$t^* = \left(\frac{\gamma_1 M_{CJ}^2 + \gamma_2}{\gamma_1 M_{CJ}^2 + 1} \frac{\gamma_2 + 1}{2\gamma_2} \right)^{-(\gamma_2 + 1)/2(\gamma_2 - 1)} t_{CJ} \tag{3.14}$$

$$x_{rf}^* = \frac{1}{\delta_{A2}} \left(\frac{\gamma_1 M_{CJ}^2 + \gamma_2}{\gamma_1 M_{CJ}^2 + 1} \frac{\gamma_2 + 1}{2\gamma_2} \right)^{-(\gamma_2 + 1)/2(\gamma_2 - 1)} L \tag{3.15}$$

The front boundary of the reflected rarefaction is known as tplateau and it is given by the relation [31]

$$t_{plateau} = t^* + x_{rf}^* / a_3 = \delta_B t_{CJ} \tag{3.16}$$

where

$$\delta_B = 2 \left(\frac{\gamma_1 M_{CJ}^2 + \gamma_2}{\gamma_1 M_{CJ}^2 + 1} \frac{\gamma_2 + 1}{2\gamma_2} \right)^{-(\gamma_2 + 1)/2(\gamma_2 - 1)} \tag{3.17}$$

The pressure at the thrust wall decays in the manner determined by interference between the exhausting rarefaction wave and its reflection from the thrust wall [33]. During the time between initial time (t=0) and the time Tplateau, the pressure at the thrust wall is kept at p_3,

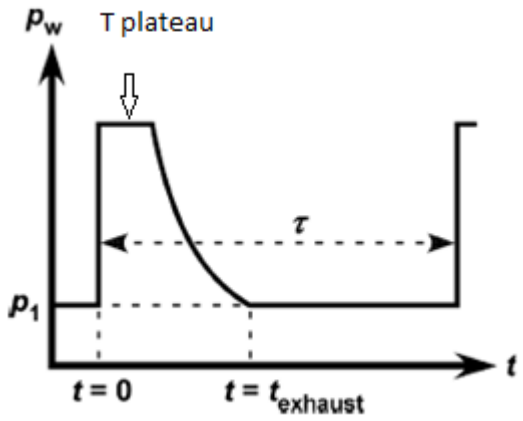

Fig 3.4: PDE cycle showing pressure history and time variation [31]

The formulation of the decay portion of the pressure history at the thrust wall is summarized in [31]. The interference between the exhausting rarefaction wave and its reflection from the closed end of the tube is considered in the following analysis.

The state of the gas inside the reflected rarefaction wave which reaches the closed end at the time Tplateau is given by [31]

$$p = \left(\frac{2}{\gamma_2 + 1} + \frac{\gamma_2 - 1}{\gamma_2 + 1} \frac{L - x}{a_3 t - a_3 t_{\text{plateau}} + L} \right)^{2\gamma_2/(\gamma_2 - 1)} p_3 \qquad (3.18)$$

$$a = \frac{2}{\gamma_2 + 1} a_3 + \frac{\gamma_2 - 1}{\gamma_2 + 1} \frac{L - x}{t - t_{\text{plateau}} + L/a_3} \qquad (3.19)$$

$$u = a - \frac{L - x}{t - t_{\text{plateau}} + L/a_3} \leq a \qquad (3.20)$$

And the quantities at the open end are maintained at the level

$$p|_{x=L} = [2/(\gamma_2 + 1)]^{2\gamma_2/(\gamma_2 - 1)} p_3 \tag{3.21}$$

$$a|_{x=L} = [2/(\gamma_2 + 1)]a_3 \tag{3.22}$$

$$u|_{x=L} = a|_{x=L} \tag{3.23}$$

In the process, when integrated into the hybrid model, these conditions are replaced by the turbine exhaust pressure to change the pressure to match the imposed back pressure from turbine exhaust.

The exhaust time is formulated as

$$t_{\text{exhaust}} = \{\delta_{A2}[f_{n'}(\delta_{A1}) - 1] + \delta_B\}t_{\text{CJ}} \tag{3.24}$$

The new approximate thrust decay history is then given by

$$a_3(t - t_{\text{plateau}})/L + 1 = f_{n'}(p_3/p_w) \tag{3.25}$$

where

$$n' = (3 - \gamma_2)/2(\gamma_2 - 1) \tag{3.26}$$

$$f_{n'}(p_3/p_w) = (1 - X) f_{n_a}(p_3/p_w) + X f_{n_b}(p_3/p_w) \tag{3.27}$$

$$X = (\gamma_2 - \gamma_a)/(\gamma_b - \gamma_a) \tag{3.28}$$

$$\gamma_a = (2n_a + 3)/(2n_a + 1) \tag{3.29}$$

In summary, the pressure history at the thrust wall is given by [32].

$$p_w(t; 0 < t \leq t_{\text{plateau}}) = p_3 \tag{3.30}$$

$$t(p_w; p_1 \leq p_w < p_3) = (L/a_3)[f_{n'}(p_3/p_w) - 1] + t_{\text{plateau}} \tag{3.31}$$

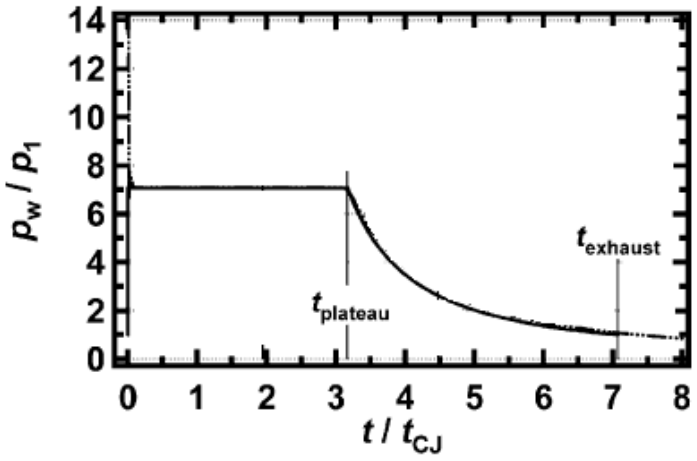

Fig 3.5: Pressure history at the thrust wall.

The performance parameters are calculated as follows [31]

The impulse per unit cross sectional area for one cycle and the specific impulse of a simplified PDE are calculated by integrating the pressure history at the thrust wall with respect to time.

$$I_{cyc} = [\delta_B + F_{n'}(\delta_{A1}, \delta_{A2})](p_3 - p_1)t_{CJ} + (p_1 - p_{out})\tau \qquad (3.32)$$

where

$$F_{n'}(\delta_{A1}, \delta_{A2}) = (1 - X)F_{n_a}(\delta_{A1}, \delta_{A2}) + XF_{n_b}(\delta_{A1}, \delta_{A2}) \qquad (3.33)$$

$$I_{sp} = \frac{I_{cyc}}{\rho_1 Lg} \qquad (3.34)$$

Phase $t_1<t<t_3$ is called the exhaust phase and after this interval, the tube is purged of residual combustion products then refilled with detonable mixture, completing the cycle at $T= T_{cyc}$ (period of cyclic operation). The interval $t_3<t<T_{cyc}$ is called purge and refilling phase. The CJ detonation properties are calculated from the NASA CEA code available from [32], rather than by equations (3.1) - (3.3) in order to properly account for the changes in thermodynamic properties such as γ and the gas constant.

The model discussed was analytically modeled in MATLAB 2010 and the results obtained are presented below for an H2/air at an equivalence ratio 1.

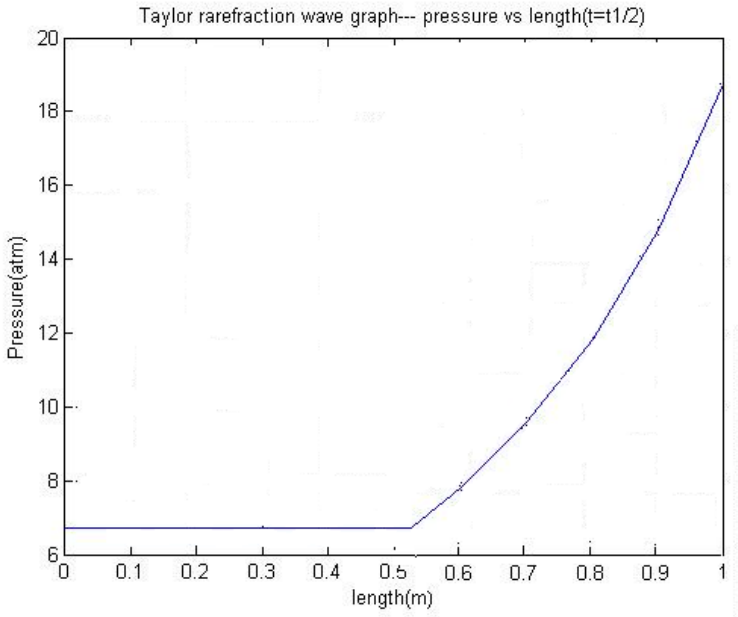

Fig 3.6: Variation in pressure as detonation wave exits tube

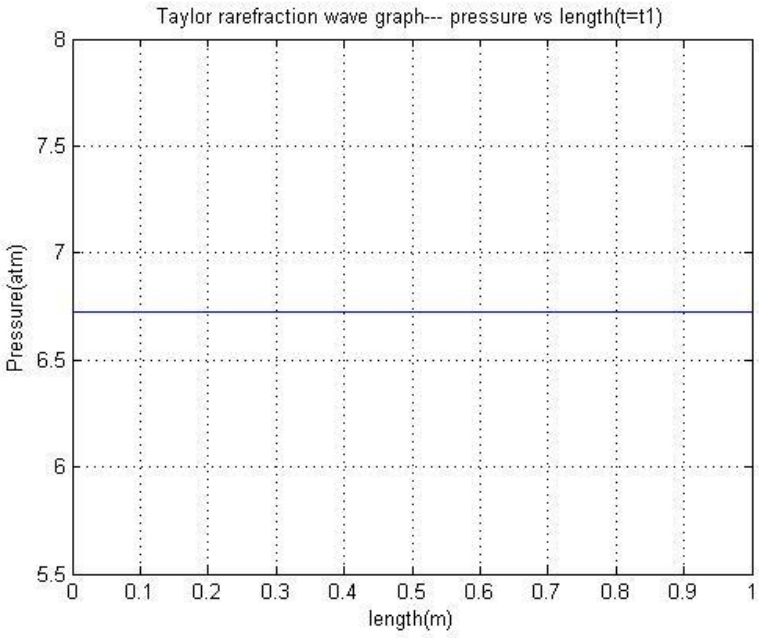

Fig 3.7: Variation in pressure as Taylor rarefaction wave exits tube

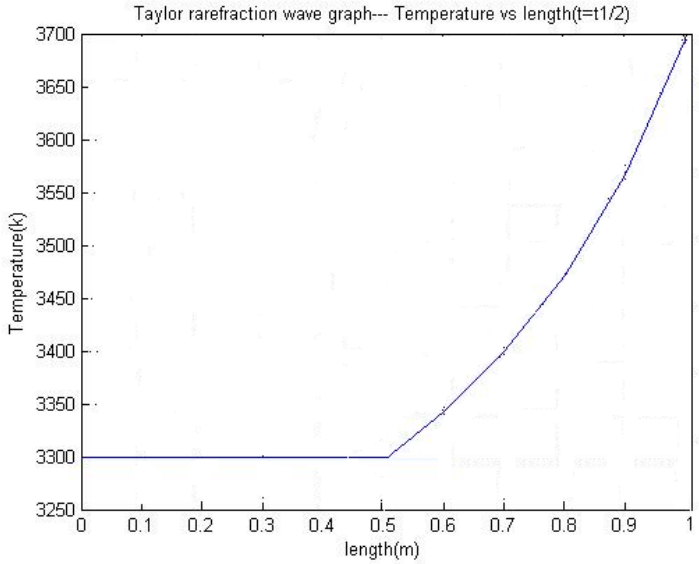

Fig 3.8: Variation in temperature as detonation wave exits tube

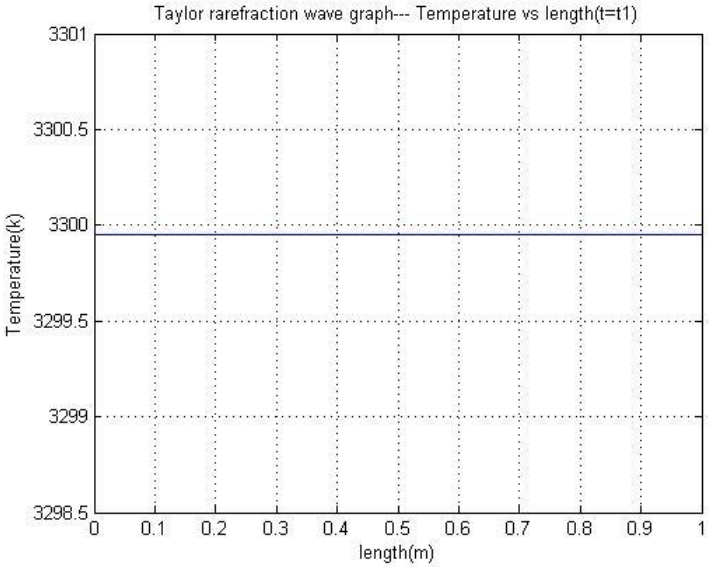

Fig 3.9: Variation in temperature as Taylor rarefaction wave exits tube

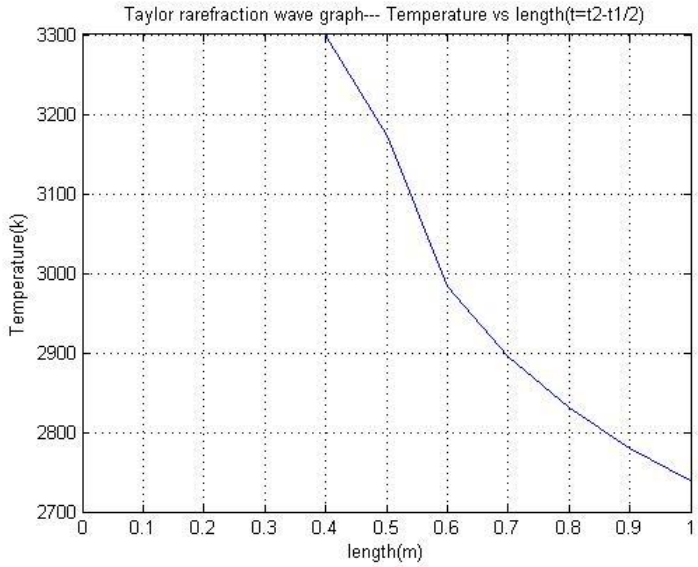

Fig 3.10: Variation in temperature during reflected rarefaction wave

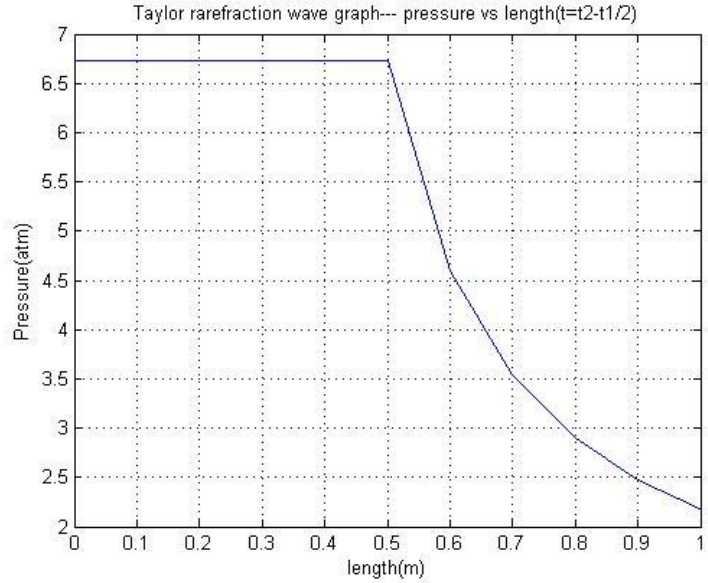

Fig 3.11: Variation in pressure during reflected rarefaction wave

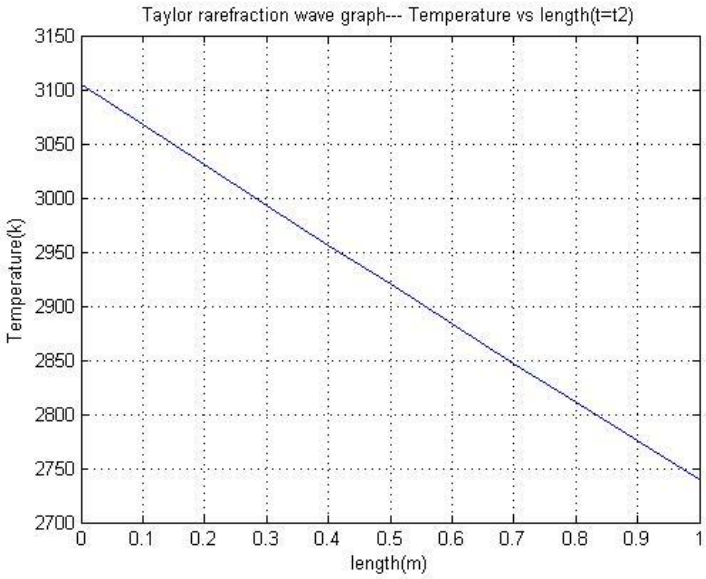

Fig 3.12: Variation in temperature at $t = t\ 2$

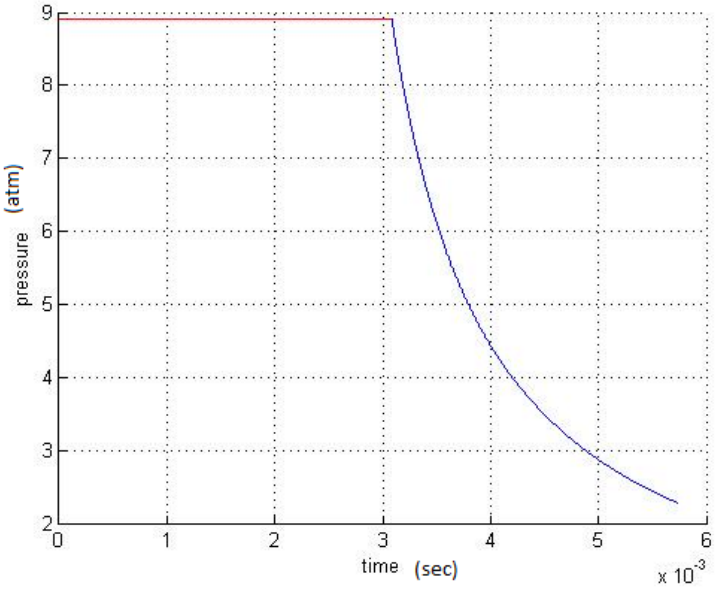

Fig 3.13: Pressure decay at the thrust wall with pressure

3.2 PDE with Different Fuels

The following section shows the variation of parameters for different fuels.

H2-Air: The following curves show the variation of frequency with the cycle time for different fuel air combinations.

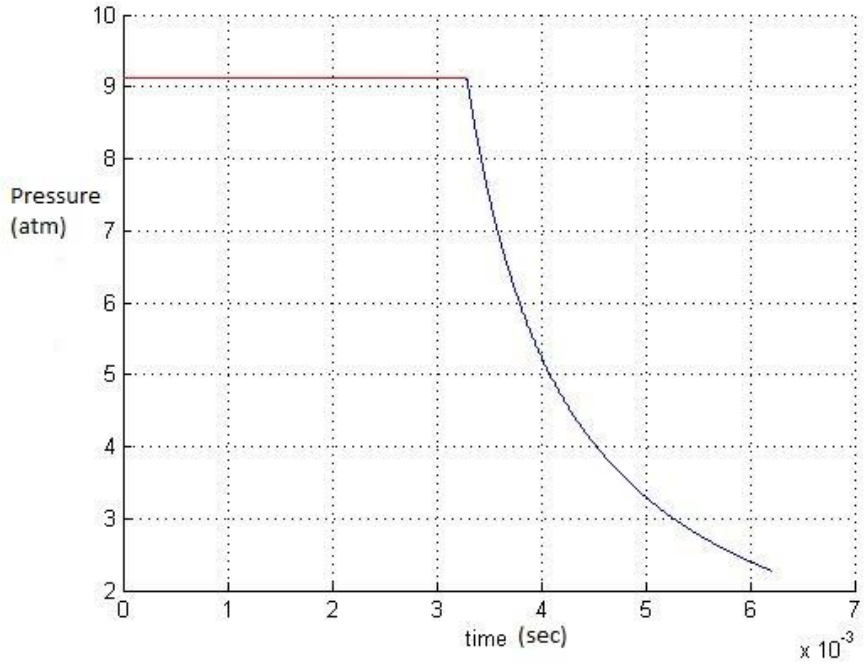

Fig 3.14: Pressure decay at the thrust wall for H2-air

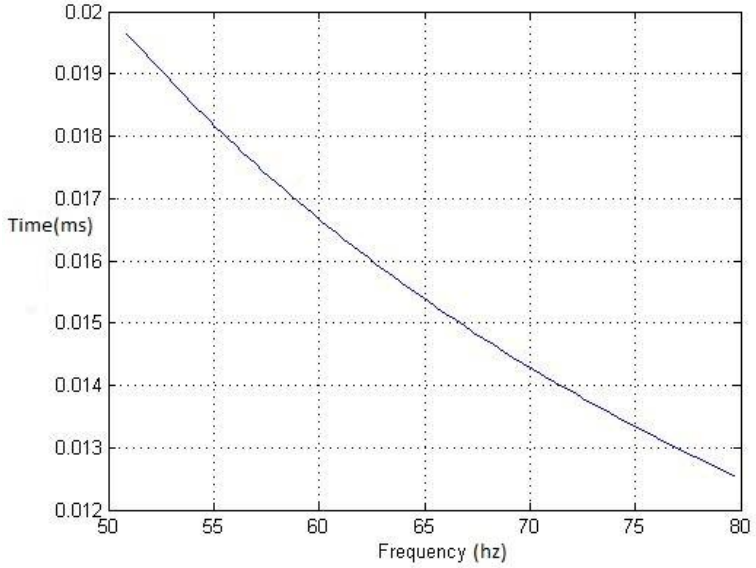

Fig 3.15: Cycle time vs. frequency for H2-air

C3H8-Air:

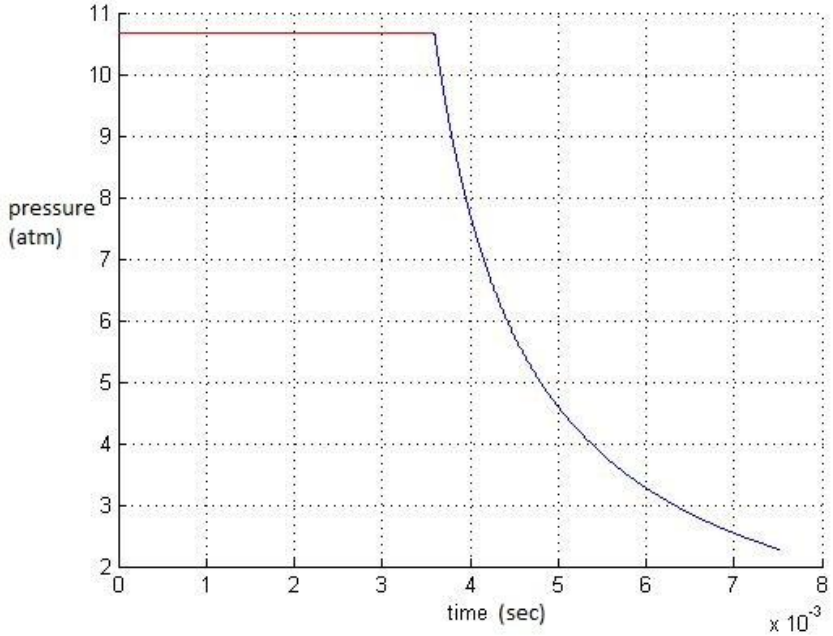

Fig 3.16: Pressure decay at the thrust wall for C3H8-air

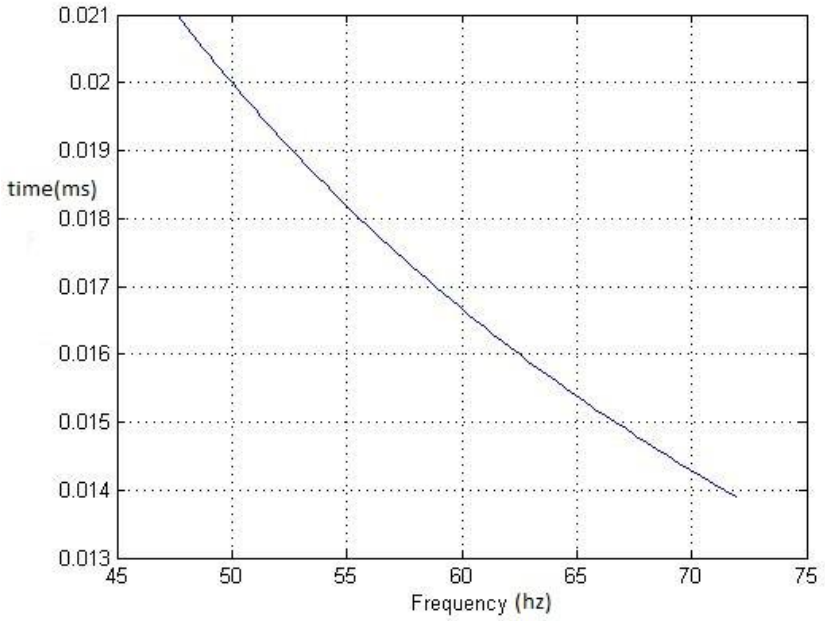

Fig 3.17: Cycle time vs. frequency for C3H8-air

CH4 –Air:

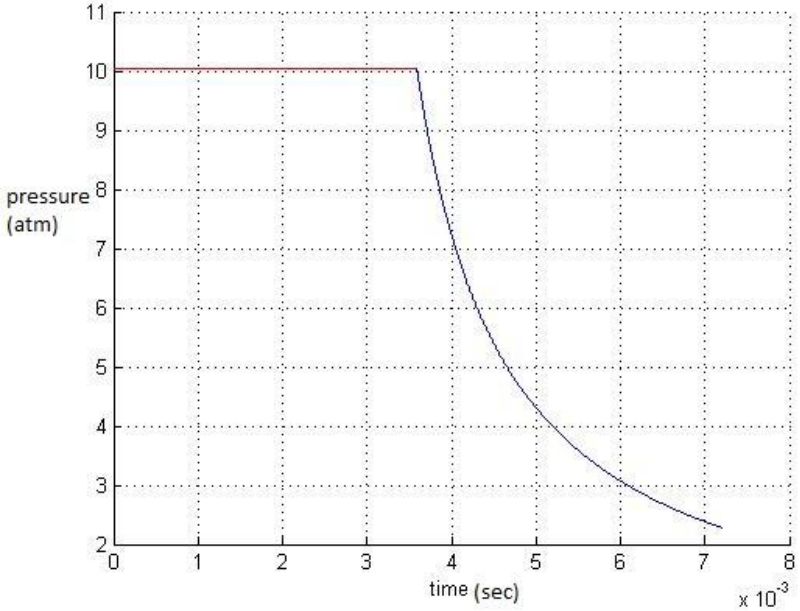

Fig 3.18: Pressure decay at the thrust wall for CH4-air

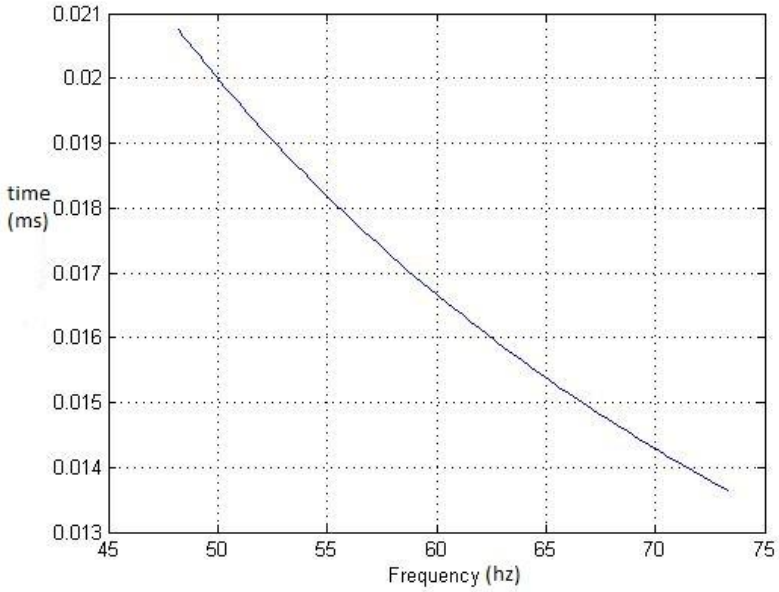

Fig 3.19: Cycle time vs. frequency for CH4-air

CHAPTER 4

ANALYSIS OF HYBRID PDE/TURBOFAN

4.1 Parametric Analysis of a Hybrid Turbofan Engine

Cycle analysis studies the thermodynamic changes of the working fluid as it flows through an engine. Parametric cycle analysis determines the performance of the engine at different flight conditions and values of design choices and design limit parameters [34].

Relating the engine performance parameters such as specific thrust and specific fuel consumption to design choices like compressor pressure ratio (Pic), fan pressure ratio (Pif) and bypass ratio (alpha) to design limitations and to the flight environment such as flight Mach number and ambient temperature is done in this chapter. Parametric analysis gives an approach to determine which engine type and component design characteristics best satisfy particular required mission requirements. The value of a parametric analysis depends directly on the realism with which the engine is characterized.

Performance trends of hybrid turbofan will be analyzed from which the basic on-design performance of the engine can be predicted. The parametric analysis of the hybrid turbofan engine helps us to look at the characteristics of several types of engines in the simplest way possible so that they can be compared.

The engine on-design process is a complex design process. Engines have a dominant influence on the aircraft's performance and are designed to cater to specific needs of the aircraft for which the engine is to be designed. Conversely, the aircraft performance requirements are also subject to the limitations in technology experienced by the engine components.

Parametric analysis curves are important for the cycle analysis of the baseline engine design, as it is easy to predict the effect of variation of the independent design parameters of the engine such as fan pressure ratio and bypass ratio on the dependent parameters such as the specific thrust and TSFC (Thrust Specific Fuel Consumption). Prediction of aircraft engine performance is one of the most significant parts of the aircraft design process

The baseline mixed flow turbofan engine without after burner was evaluated with PARA software provided by Mattingly's Aircraft Engine Design text [34]. Once the baseline engine and the results from the PDE tube where obtained, implementing the hybrid model and analysis are presented in the following section.

Component efficiencies are selected from Mattingly's Table 4.4 [34], using level 4 technology.

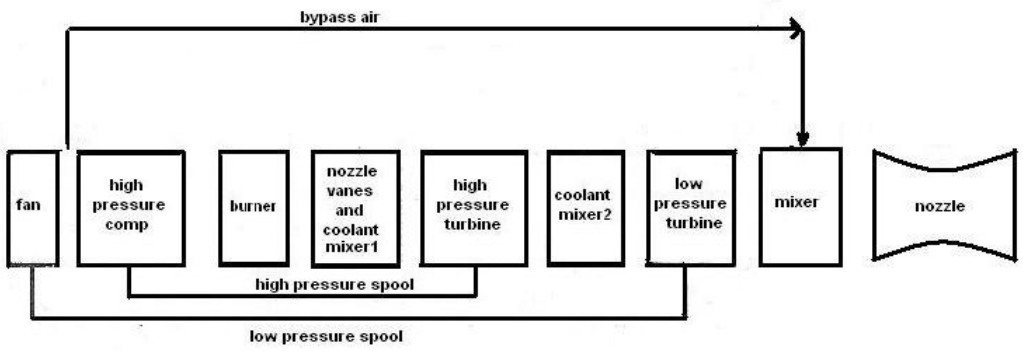

Fig. 4.1: Mixed flow turbofan engine

Baseline mixed flow turbofan engine:

A schematic of the mixed flow turbofan engine is described in Fig 4.1. This figure illustrates a 2-spool, low-bypass turbofan engine with a mixed exhaust, showing the low-pressure and high- pressure spools. The fan is driven by the low-pressure turbine; whereas the high-pressure compressor is powered by the high-pressure turbine. The engine employs a mixed flow stream. A mixer is incorporated to mix the flow from the turbine and the fan bypass

before exiting into the afterburner or nozzle. Idealized engine components are assumed in that the working fluid behaved as a perfect gas with constant specific heats. The baseline mixed flow turbofan was modeled mathematically in MATLAB described by Mattingly [34]. The engine was first modeled in PARA [provided by Mattingly's Aircraft Design software] with input parameters for the cruise conditions.

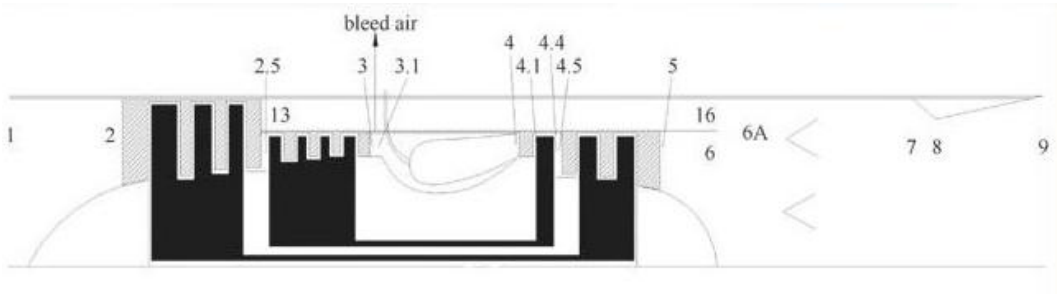

Fig. 4.2: Schematic of mixed flow turbofan engine [34]

Hybrid turbofan with PDE tubes in the Bypass duct:

The hybrid turbofan is similar to the baseline engine, but the bypass section is replaced by a series [6-8] of PDE tubes detonating out of phase. The core of the turbofan engine remains unaffected by the detonation combustion in the bypass duct [34]. After the detonation chambers are filled with fuel-air mixtures through rotary-valves, detonation is initiated and after the blow-down process, purging of residual combustion products occurs before injecting a new mixture. The exhaust from the PDE goes in to the mixer section. Realistic performance estimates can be predicted by CFD results as done in Ref [36], but simple analysis can be carried out for parametric studies to predict basic performance. In this pulse detonation engine concept the after burner is eliminated. Addition of PDE tubes in the bypass duct will increase overall engine weight and will increase total pressure losses of the bypass duct airflow [35] and increases the pressure ratio of the bypass flow. The PDE tubes detonate out of phase. The number of tubes detonating at a time will predict the cycle time and frequency.

In this thesis the nominal PDE is a 1 meter long tube without a nozzle placed in the bypass duct of a mixed flow turbofan. The performances of different detonable mixtures are considered in the analysis. Specific thrust, TSFC and thrust can be calculated as functions of compressor pressure ratio of the engine, fan pressure ratio, bypass ratio, length of the PDE tubes and equivalence ratio.

Initially the tube is assumed to be with filled with an H2-air mixture. The initial temperature and pressure depends on the altitude, Mach number and fan pressure ratio. The equivalence ratio is assumed to be unity. As discussed in the previous chapter the pressure at the thrust wall rapidly decays after the detonation wave exits the tube and the blow down process is initiated.

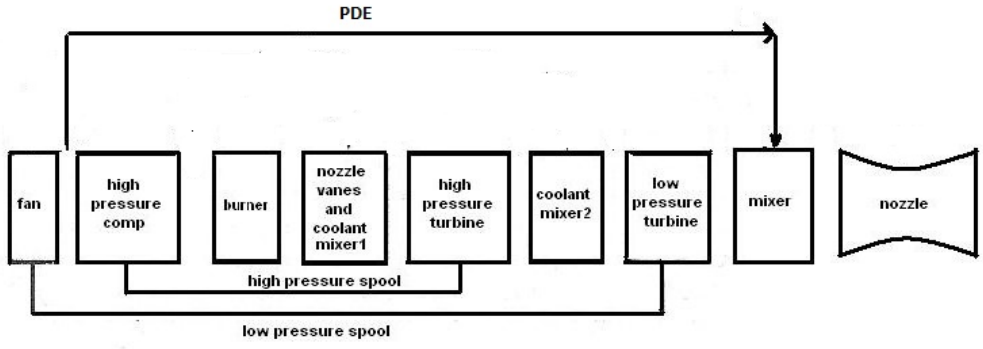

Fig 4.3: PDE tubes in the bypass of the mixed flow turbofan

The pulse detonation turbofan analysis is done to predict the performance of the engine. The performance of the baseline turbofan engine is calculated using Mattingly's approach for mixed flow turbofan engine. The pressure history at the thrust wall is predicted by the method described in the previous chapter. The exhaust pressure and temperature from the bypass PDE is calculated by taking the average values of the pressure and temperature history during the complete detonation cycle. The Mach number is determined by the total pressure ratio Pt16/Pt6. Since the turbofan cycle has three design parameters, compressor pressure

ratio, fan pressure ratio and bypass ratio, its performance can be best understood by performing a parametric variation of these design parameters.

To demonstrate the potential performance gain using the pulse detonation engine/turbofan, the values of specific thrust and thrust specific fuel consumption are predicted. The filling time was varied, in turn changing the frequency. Equivalence ratio and tube lengths were varied to see the performance of the hybrid engine. Results demonstrate the performance benefits of using the pulse detonation turbofan engine concept.

Designing the engine involves the detailed designing of each of these components. But prior to the component design, an overall engine design has to be pursued to determine the engine 'design point' cycle parameters. One of the aims of this thesis is to understand the various issues involved in hybrid engine selection and design. The number of engine components and the thinking behind the higher level design also differs according to the engine class.

The figures presented in the results chapter, explain the performance trends of a hybrid turbofan engine. Increasing the compressor pressure ratio increases the thermal efficiency. Decreasing the fan pressure ratio reduces exit velocity and increases propulsive efficiency. Once the promising ranges of these parameters have been found, off design or performance analysis can be proceed and selected engine sized to produce the installed thrust required [35].

Parameter On-Design Choices:

The design choices listed in table 4.1 below used for the analysis above are based on a parametric study performed with the hybrid mixed flow turbofan model at design conditions. Changes in these design parameters may improve engine performance at design and/or off-design conditions. Finding the right combination for a given task requires ingenuity and persistence, and it is not even certain that a successful combination can be found. Inputs for the process have been arranged in order of increasing designer control by greater possible range of variation [35]. With respect to the parameters, there would be vast array of possible outputs, and a judicious selection must be made. A search was conducted to find the influence of each of the design parameters and from that the combination that work well at each of the flight conditions. Examining the engine behavior at extreme conditions at which the engine plays greatest role in constraint or mission analysis [34]. In order to narrow down the key engine design parameters investigation of possible combinations of design points at selected critical flight conditions are done. To reduce the large number of promising reference point choices to manageable size, a few critical flight conditions having significantly different characteristics may be used to establish important trends. In this case for a cruise condition at 0.9M at 35-40kft was taken as the reference and design parameters for cruise were investigated.

Table 4.1: Parametric Design choices

Compressor Pressure ratio	24
Fan pressure ratio	3.8
Alpha	1
TT4 Mach number	1777k 0.9
Altitude	36000ft
Length of the PDE tube	1

Results at the design point:

Baseline mixed flow turbofan engine: F/m_0 = 778.14 N/kg/sec

S = 21.61 mg/sec/N

The performance for the baseline hybrid PDE/Turbofan with different fuel/air mixtures at the same flight conditions is summarized below:

DP (H2+air) Hybrid PDE turbofan engine:

$F/m_0 = 888.76$ N/kg/sec

$S = 31.48$ mg/sec/N

DP (C3H8+air) Hybrid PDE turbofan engine:

$F/m_0 = 908.24$N/kg/sec

$S = 31.77$ mg/sec/N

DP (CH4+air) Hybrid PDE turbofan engine:

$F/m_0 = 890.05$ N/kg/sec

$S = 33.36$ mg/sec/N

4.2 Mixer Analysis

Mixed flow turbofan engines are most commonly used for military applications, and generate higher specific thrust. However the higher specific thrust would mean lower propulsive efficiency, giving higher specific fuel consumption. The mixing of the two streams in a mixed flow turbofan engine offers performance gain but with a small loss in total pressure because the enthalpies of the two streams are redistributed [34]. The reason for the impact of the mixer on the performance of the engine is that the fan and core streams are not separately exhausting to the atmosphere, and they are bought together in pressure contact within confined quarters [34]. There are situations that arise in the mixer model where there could be reverse flow in the fan

bypass duct (M16 less than zero), or the flow may become choked at the mixer exit [M6A greater than one]. Common practice is to keep the design point values of M6 and M16 in the range of 0.4-0.6[34]. The design variables such as compressor pressure ratio (Pic), fan pressure ratio (Pif), and bypass ratio (alpha) are balanced so that M16 not be less than zero or M6A greater than one. The Kutta condition requires equal static pressures at stations 6 and 16. Normal design of the mixer has the Mach numbers of the two entering streams nearly equal. When the optimum fan pressure ratio is achieved it is assumed that *p*016/*p*06 =1. This condition is not always fully satisfied. The value of the ratio *p*016/*p*06 rises for off-design conditions. If the value is greater than one at design point, serious mixing losses may result at off design operations. Therefore, we choose the value of *p*016/*p*06 between 0.95 and 1 at the design point even if it is slightly sub optima at that particular operating point. Varying compressor pressure ratio in the cycle analysis is done so that it matches the product of the fan pressure ratio and the cycle-average PDE pressure ratio. When *p*016/*p*06 is close to one, the loss (entropy generation) due to mixing would be small.

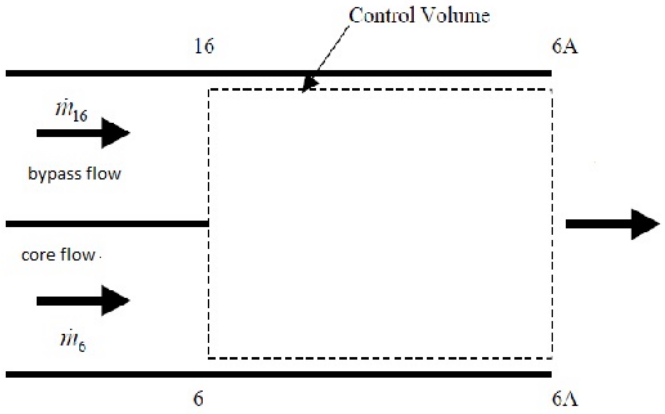

Fig 4.4: Baseline turbofan Mixer analysis

Hybrid PDE Mixer Analysis:

The design point flight conditions are same for the mixed flow Hybrid PDE/turbofan engine. As mentioned above the value of M16 can't be less than zero (reverse flow) or M6A greater than one (choked flow). The bypass ratio and fan pressure ratio are selected through parametric analysis in such a way that these conditions are satisfied. The frequency of the PDE tube has a major impact on the pressure and temperature released from the tube to the mixer inlet, and affects the thrust and specific fuel consumption.

It was observed that for a various combinations of particular fan pressure ratio, bypass ratio and compressor pressure ratio, the value of M16 or M6A exceeds 1 and conditions weren't satisfied for the mixing model. The values of all those parameters were selected in such a way that they match all the requirements for the mixing process. The average values of pressure and temperature are directly proportional to the frequency of the PDE tube. As the frequency increases both the cycle averaged pressure and temperature expelled from the PDE tube increase, increasing the total pressure ratio and M16, therefore increasing the risk of choking as M6A was approaching 1.

The cycle averaged exhaust pressure is calculated from

$$P(avg) = (1/T)^* \int P(t)\, dt$$

From pressure plots as shown in the Fig 4.6 .P (avg) is a function of frequency (Hz). The same procedure is used to calculate the average temperature and it is also is a function of frequency (Hz). The temperature drops to the fan exhaust temperature when purge air is injected into the PDE combustion chamber. The purge would be accomplished by opening the valve and injecting fan discharge air to remove residual combustion products prior to injecting the next pulse of fuel.

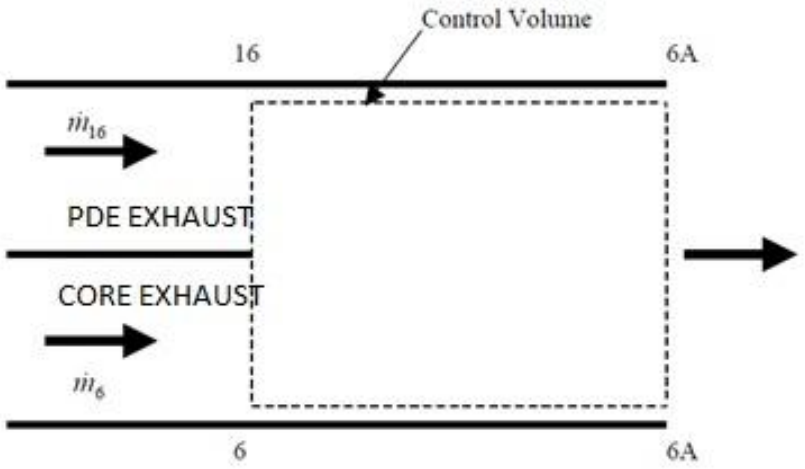

Fig 4.5: Hybrid PDE mixer analysis

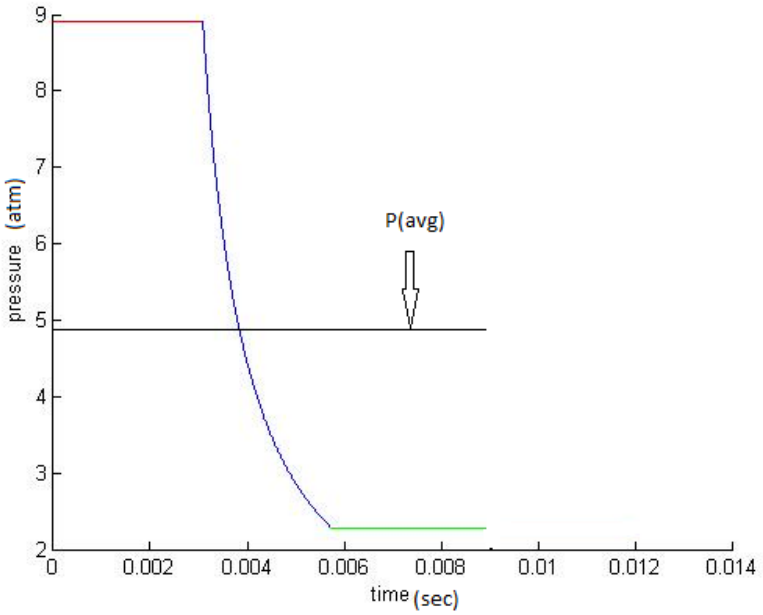

Fig 4.6: Pressure history at thrust wall for Baseline Hybrid turbofan engine for 110 Hz

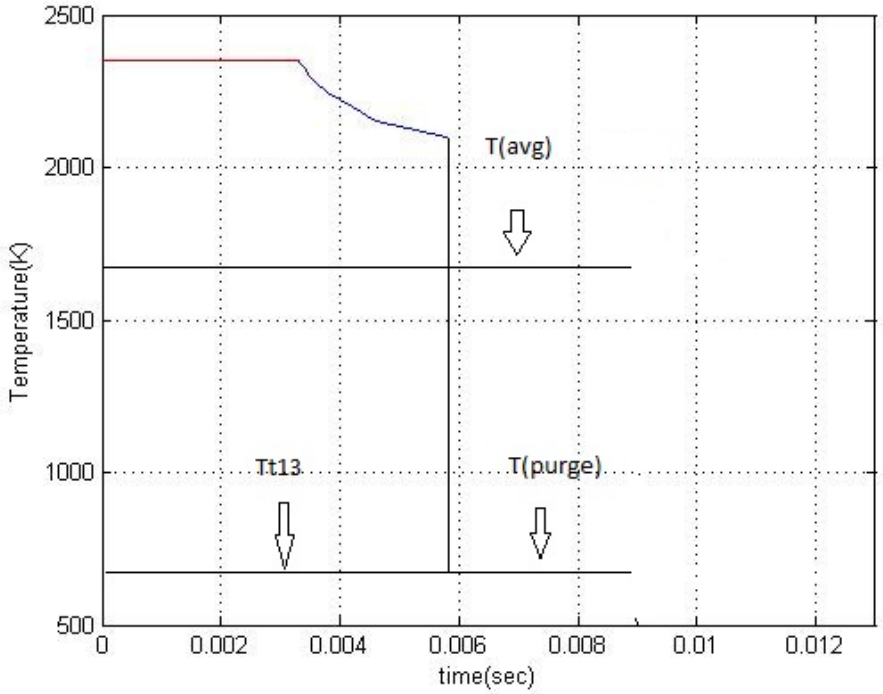

Fig 4.7: Temperature history at thrust wall for Baseline Hybrid turbofan engine for 110 Hz

Case (1):

P (avg) = 4.96 atm

T (avg) = 1675 k

Frequency= 110.00 Hz

M16=0.49

F/m_0=869 N/kg/s

S=34.42mg/s/N

Pt16/Pt6=1.05

Case 1 shows the conditions from the PDE exhaust entering into the mixer for the frequency of 110 Hz. The average pressure decreases with an increase in cycle time, as does the temperature entering into the mixer. The cycle time is increased by increasing the purge and refill time of the cycle, therefore changing the average flow conditions entering in to the mixer.

This yields change in specific thrust and specific fuel consumption. For case 1 the frequency was set at 110 HZ, which yielded the specific thrust of 869.1 N.s/kg and specific fuel consumption of 32.42mg/s/N

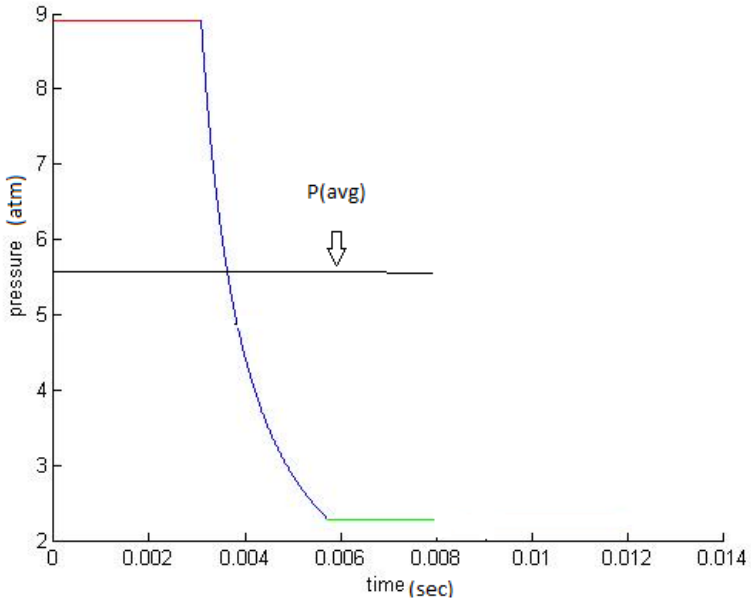

Fig 4.8: Pressure history at thrust wall for Baseline Hybrid turbofan engine for 125 Hz

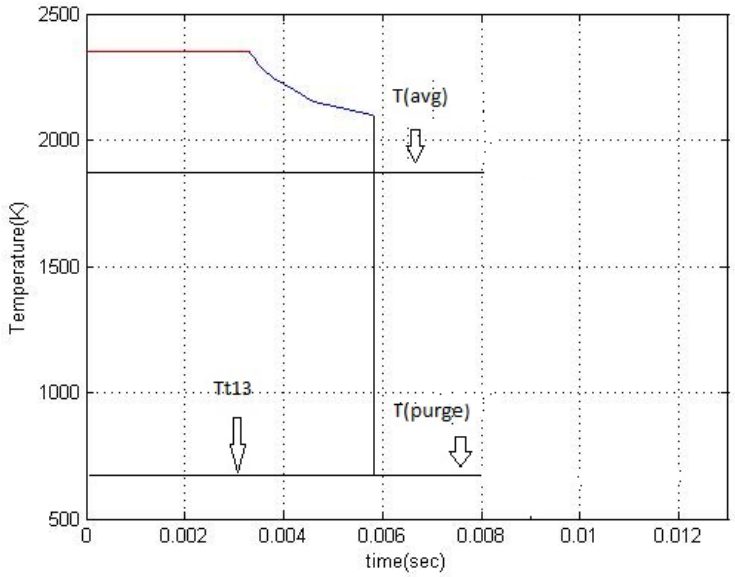

Fig 4.9: Temperature history at thrust wall for Baseline Hybrid turbofan engine for 125 Hz

Case (2)

P (avg) = 5.57atm

T (avg) = 1850 k

Frequency = 125 HZ

M16=0.5124

F/m_0=874.8 N/kg/s

S= 32.73mg/s/N

Pt16/Pt6=1.18

Case 2: The frequency was set at 125 Hz; this was done by decreasing the cycle time which yielded a higher average pressure and temperature entering into the mixer. The increase in frequency shows a higher in specific thrust compared to case 1. As the frequency increase the performance of the baseline hybrid engine increases over the baseline mixed flow turbofan engine.

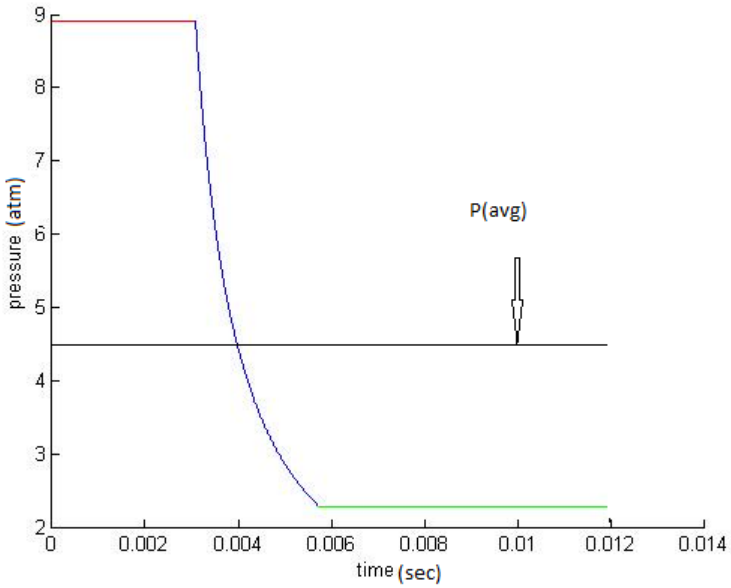

Fig 4.10: Pressure history at thrust wall for Baseline Hybrid turbofan engine for 83 Hz

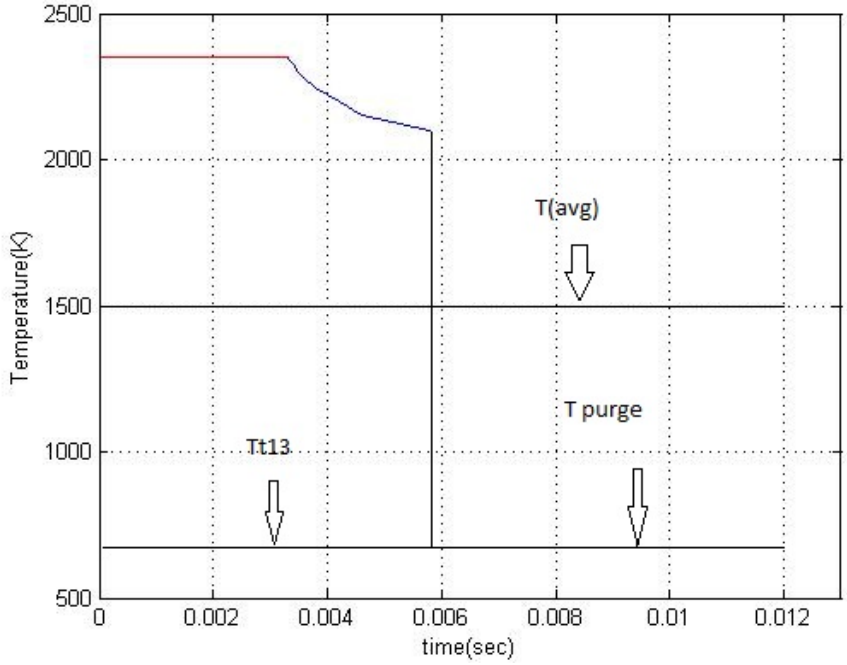

Fig 4.11: Temperature history at thrust wall for Baseline Hybrid turbofan engine for 83 Hz

P (avg) = 4.53 atm

T (avg) = 1507 k

Frequency = 83.00 HZ

Pt16/Pt6<1

Case 3: the frequency is set to a lower value of 83 Hz .The ratio of pt16/Pt6 yielded a value of 0.7649 and which is significantly less than 1, the frequency is not suitable for the mixing process because of the reverse flow in the system i.e., M16<0.

The effect of frequency on the specific thrust and specific fuel consumption is given by the figures below

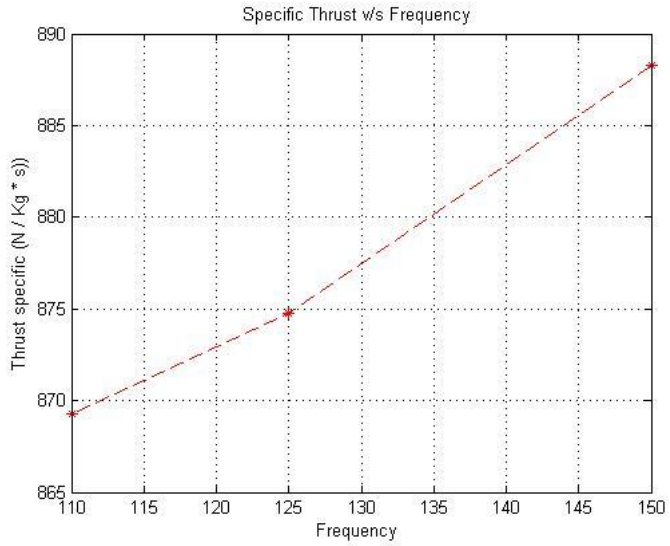

Fig 4.12: Effect of frequency on specific thrust

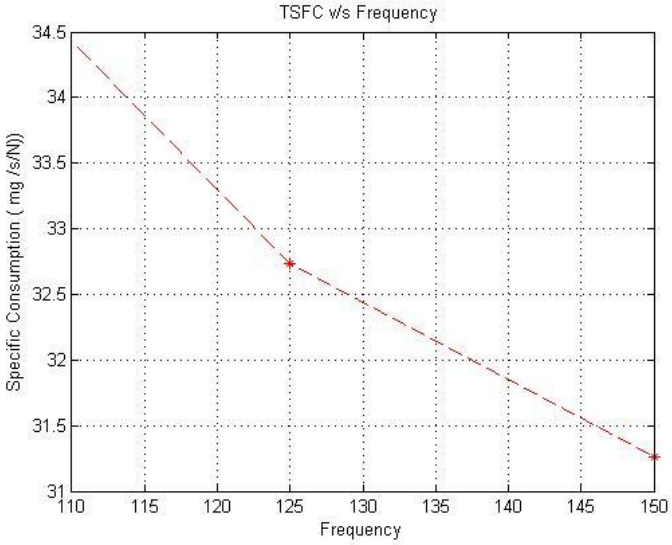

Fig 4.13: Effect of frequency on specific fuel consumption.

For the baseline hybrid case predicted, the pressure expelled out of the PDE is calculated by the averaging the variation of PDE exhaust pressure vs. time. The same procedure is used for the average exhaust temperature. The average values are found and the

ratio of Pt16/Pt6 is calculated for hybrid engine and later on used for the calculation of M16 (<1). In the case of baseline hybrid engine Pt16/pt6 is 1.2372 and the values of M16 is 0.6872.

The range of alpha for hybrid engine is 0.8-1. Fan pressure ratio can varied from 3.6-5.4.Compressor pressure ratio varies from 20-30. The range of Pt16/Pt6 and M16 are limited for mixing to occur without the flow is being choked or having reverse flow. The allowable frequency ranged from 85-165 Hz.

4.3 Performance Analysis of a Hybrid Turbofan Engine

Baseline Turbofan Off-Design Performance:

Performance analysis determines the performance of a specific engine at all flight conditions and throttle settings. The objective of this analysis is to determine the engine's performance over its operating envelope [34]. Once an engine cycle with design choices is selected, the results of performance analysis are used to predict its off design performance. The mixed flow turbofan has good fuel efficiency when operated with the after burner off, and high specific thrust when it's turned on. The mixing of the core stream and bypass stream in the fixed area mixer adds six additional dependent variables to the performance analysis. Since the static pressure at stations 6 and 16 must be equal, the total pressure ratio of the two streams will be near unity. This dramatically restricts the fan pressure ratio and bypass ratio for this type of engine.

Off-Design Assumptions

The off-design modeling used by Ref. [34] uses the following assumptions:

- The flow is assumed to be choked at high pressure turbine entry, low pressure turbine entry and at the nozzle throat.
- All component efficiencies other than the inlet are assumed to be constant at all operating points. Burner, afterburner and nozzle pressure ratios are also same on and off design.
- Gas properties are that of calorically perfect gases. C_{pt} is allowed to vary with bypass ratio.
- P_0/P_9 is assumed adjustable by changing exit area.
- The engine dimensions are same as at design point everywhere except at the throat and exit of the nozzle.

At the beginning of the off-design analysis a design point is chosen such that it falls within the range specified by the on-design analysis. This engine is referred to as the base-line engine [2]. Now one design choice at a time is varied over the range, keeping all other parameters constant. With the variation of the design choices many different performance variations are generated. The engine which predicts best performance for a particular parameter is considered and the remaining parameters are varied. As a result, step-wise we can obtain optimum values of design choices for which the engine shows best performance [35].

Hybrid Turbofan Engine Off-Design Performance:

The same procedure is carried out with the hybrid PDE/Turbofan. The only difference is the cyclic averaged pressure and temperature from the PDE tube, which will have a major impact on the performance of the engine. The total temperature ratio and Mach number at the exit of the bypass duct entering the mixer is mainly dependent on the conditions the engine is

flying in and the design parameters are iteratively determined for matching the conditions which can avoid mixing problems during the whole flight mission. The final engine will always be running off design and will therefore behave differently at each operating point, thus finding an engine with fixed design point parameters that works well at every operating point is a challenging task. The performance of the hybrid turbofan engine was determined over a range of off-design conditions, at various Mach numbers, altitudes and compared to that of the baseline engine.

CHAPTER 5

RESULTS

The area of the PDE tube and the inlet Mach number determine the time required to fill the tube, which controls the frequency [45] and thus the cycle averaged thrust. It was anticipated that low bypass turbofans is more effective at the cruise conditions than any other in flight condition by analysis it appears that inlet Mach number 0.9 is most beneficial at altitude 36000 ft. is more productive for hybrid PDE/Turbofan engine compared to the mixed flow turbofan engine.

Figure 5.1 shows the results of the most promising combinations of design choices. The specific fuel consumption is plotted in order to allow for convenient comparison of the influence of the various engine design parameters. Figure 5.1 shows that specific fuel consumption and specific thrust mainly depend upon bypass ratio (alpha) and compression pressure ratio (Pic) increasing alpha alone increases specific thrust. Fan pressure ratio increases with compressor pressure ratio and turbine inlet temperature, and decreases with alpha. Specific thrust and specific fuel consumption decreases with increase in alpha alone, so the value of alpha in the range or 0.6-1 would be best for this flight condition. The maximum value of specific thrust is due to increasing values of compressor pressure ratio [35], and increasing Pic maximizes the specific thrust and decreases specific consumption. Therefore compressor pressure ratio is held in the range of 20-30 for this flight condition. A thorough parametric study should be conducted to identify such design parameters as number of tubes, tube geometry, etc., that may yield better performance at on design and off-design conditions.

Increasing the compressor pressure ratio decreased the specific fuel consumption and increased the specific thrust of the engine. The figures show the trends of hybrid engine with respect to the baseline engine at cruise conditions, Mach 0.9 and altitude 36000 ft**.** Figures 4.12 and 4.13 of the previous chapter show how varying equivalence ratio affects the net thrust and TSFC.

At sea level the hybrid engine has a 12.9% increase in specific thrust over the baseline engine. Whereas the hybrid engine at Mach 2 and 45,000 ft has a 6.2% increase in specific thrust, but the TSFC increased by 3.9%. The variations of the engine with respect to the flight Mach number are presented in Fig 5.12- 5.15. The variation of specific thrust and fuel consumption are plotted below. Shorter tube lengths increased the frequency and in turn produced more thrust while decreasing the specific fuel consumption. Tube diameter is considered to be constant throughout. The variation of tube diameters with length is not considered in this thesis.

The design of the Hybrid PDE/Turbofan has been optimized after the parametric analysis and was evaluated for potential improvements. The configuration at the cruising conditions allowed the thrust increase by 11.8% for the baseline hybrid PDE/Turbofan engine.

Results of Parametric analysis:

Figs 5.1-5.3 show the parametric variation of specific thrust vs. specific fuel consumption for varying compressor pressure ratio [from 8 to 24] and bypass ratio from zero to one. These graphs are base for predicting the baseline hybrid PDE/Turbofan engine. Varying a parameter checking the performance trends, holding one parameter and changing the other parameter to obtain a best combination for the hybrid engine was done and the parameters for the baseline was predicted as shown in section 4.1.

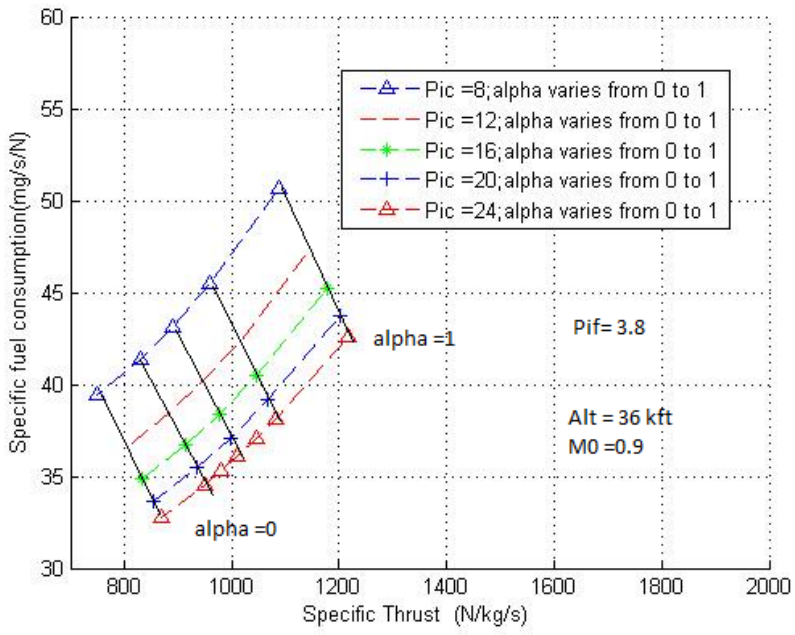

Fig 5.1: Parametric analysis for baseline Hybrid engine (H2/air)

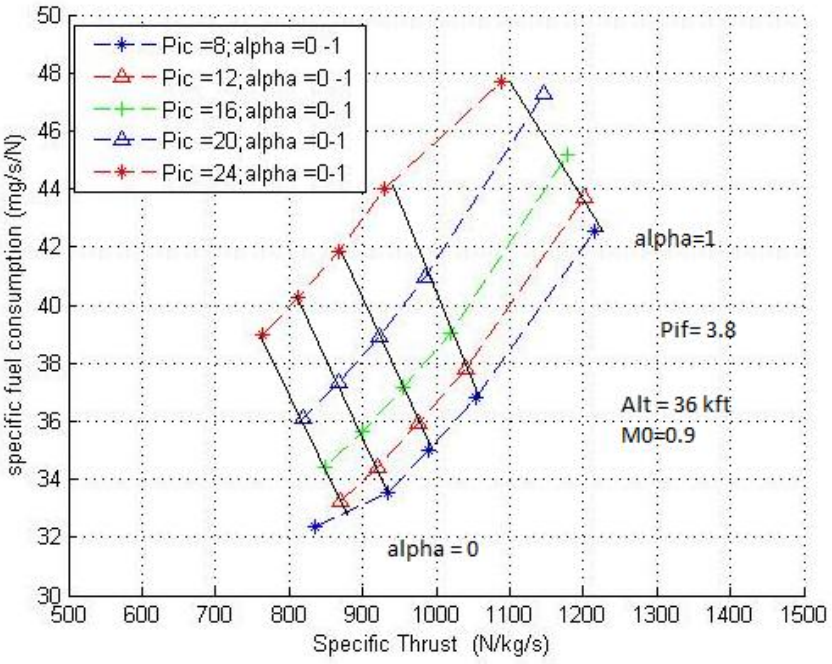

Fig 5.2: Parametric analysis for baseline Hybrid engine (C3H8/air)

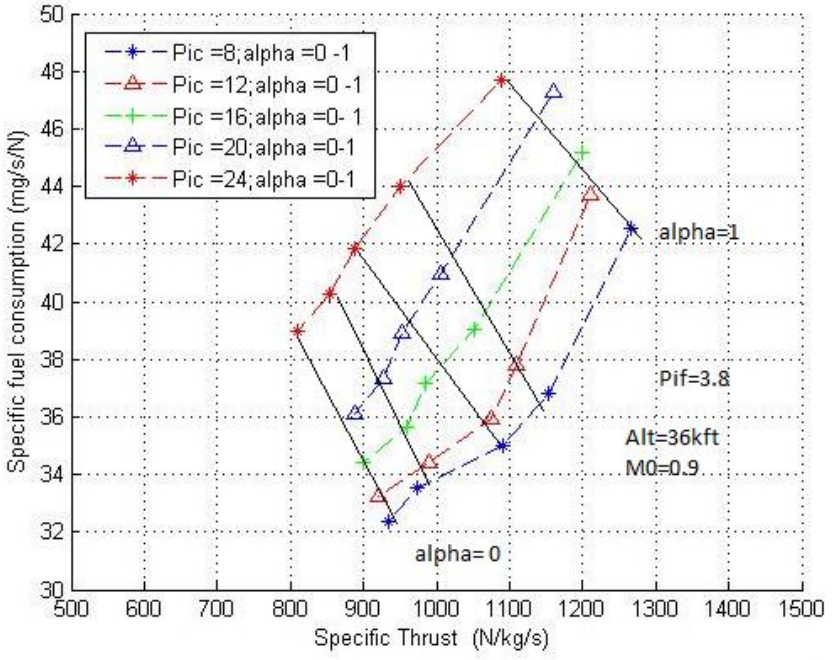

Fig 5.3: Parametric analysis for baseline Hybrid engine (CH4/air)

Figs 5.4-5.6 show the comparison of the baseline hybrid PDE/Turbofan with the baseline mixed flow turbofan engine. Fig 5.5 shows the trend of specific thrust with specific fuel consumption, which clearly predicts the performance gain of the hybrid engine over the turbofan engine. Fig 5.5 presents the trend of specific thrust with varying compressor pressure ratio, which shows higher thrust for the hybrid engine at the same operating conditions. The specific fuel consumption trend is shown in Fig 5.6, predicting higher fuel consumption compared to baseline mixed flow turbofan engine. Figs. 5.7 - 5.9 shows the performance of the hybrid engine with respect to the length of the PDE tube in the bypass duct of the hybrid engine. As shown in the figures the specific thrust of the hybrid engine increases as the length of the tube increases and the specific fuel consumption decreases.

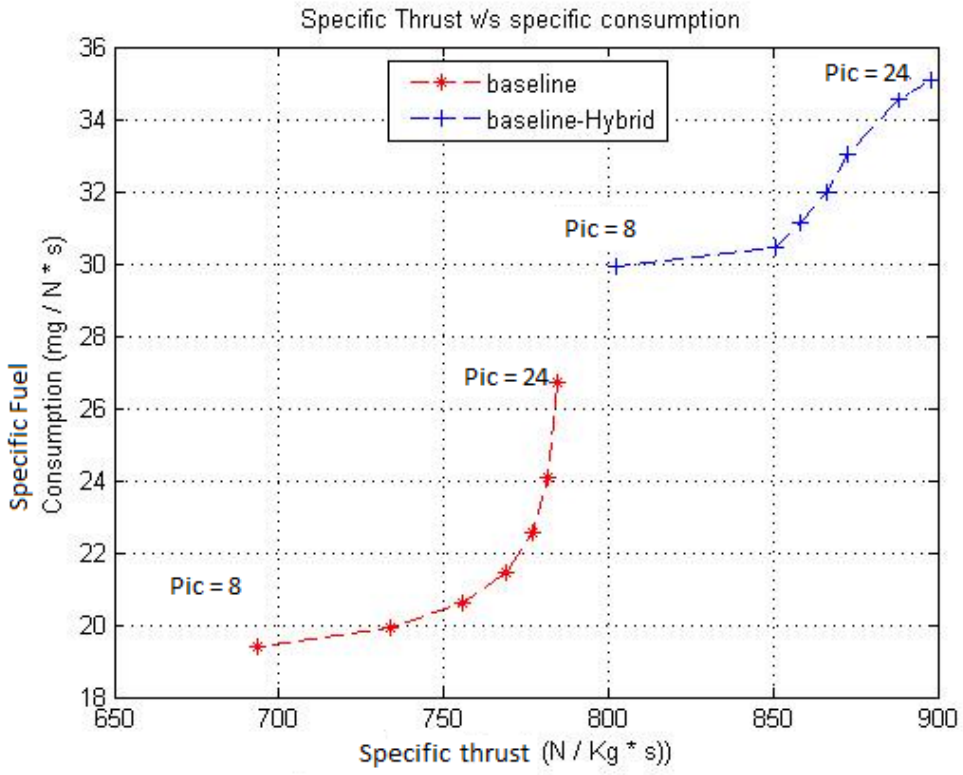

Fig 5.4 Baseline hybrid performance: Specific fuel consumption vs. Specific thrust for varying compressor pressure ratio.

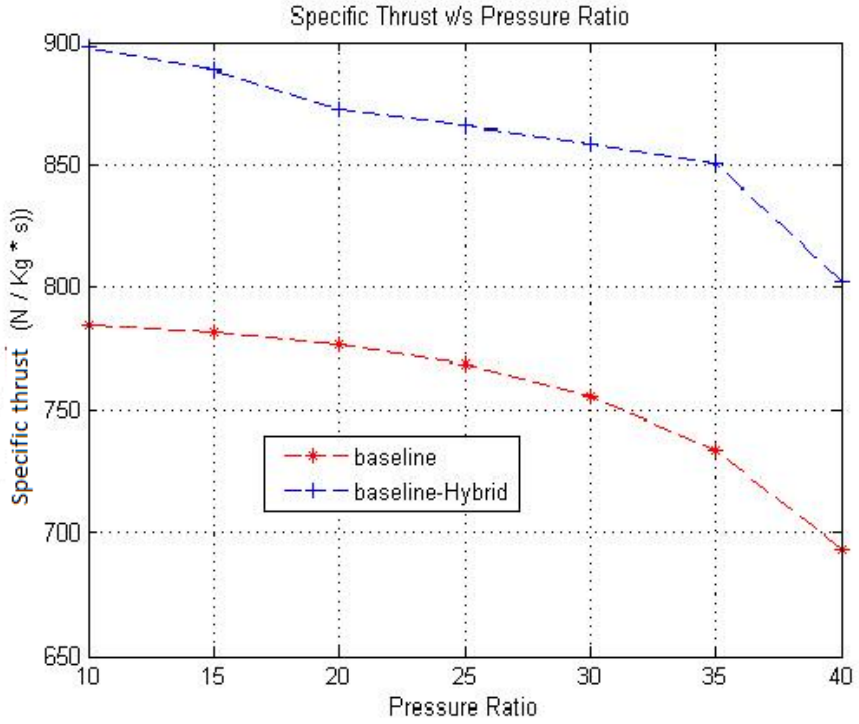

Fig 5.5: Baseline hybrid performance: Specific thrust for varying compressor pressure ratio.

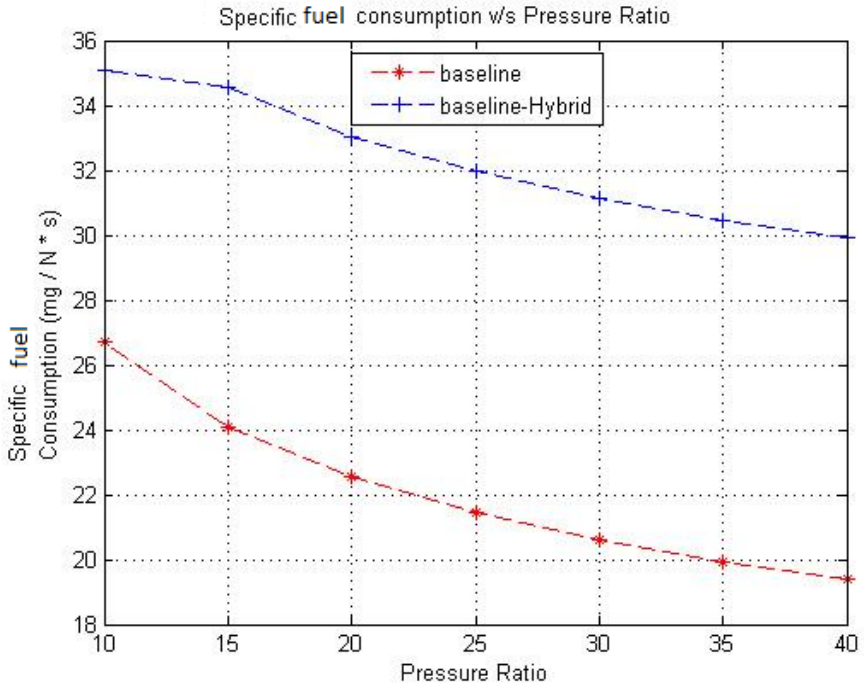

Fig 5.6: Baseline hybrid performance: TSFC for varying compressor pressure ratio.

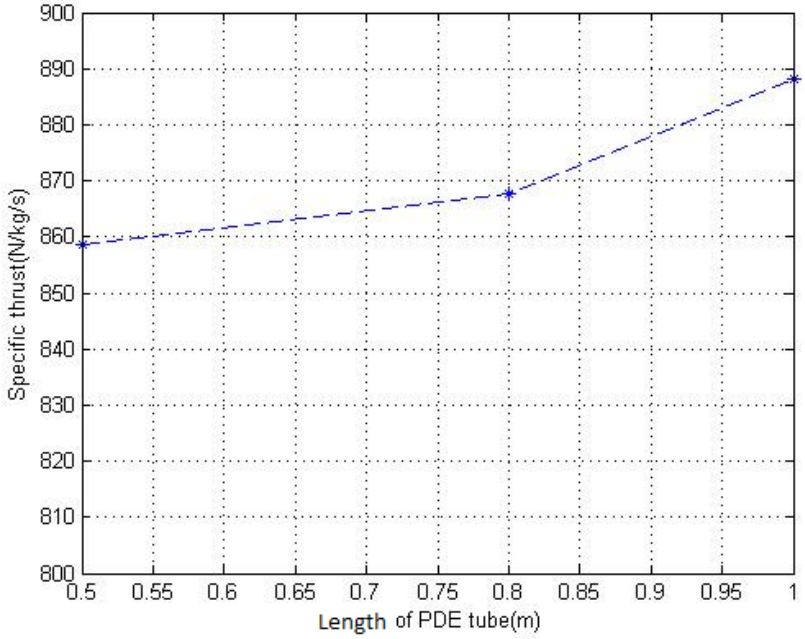

Fig 5.7: Baseline hybrid performance: Specific thrust vs. PDE length.

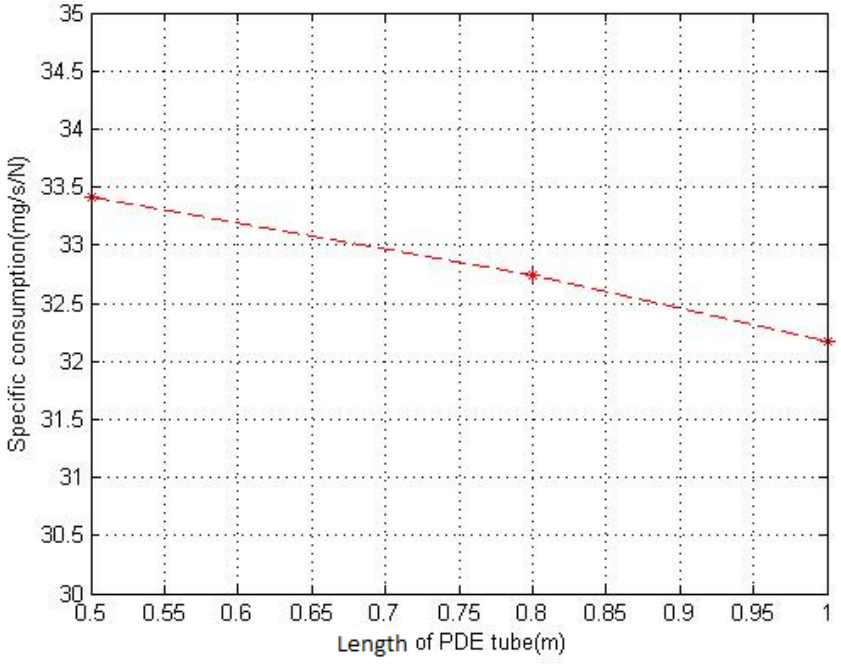

Fig 5.8: Baseline hybrid performance: Specific thrust vs. PDE length.

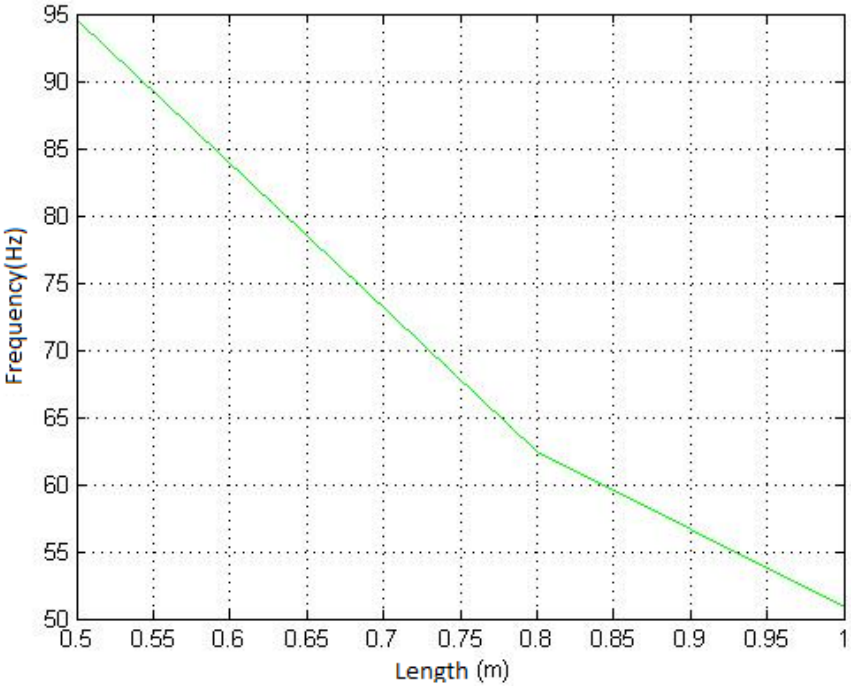

Fig 5.9: Frequency vs. PDE length.

The effect of equivalence ratio on the performance of the hybrid PDE/Turbofan engine concept was predicted by varying the overall mixture equivalence ratio. Fig 5.10 and 5.11 show the trend of specific thrust and specific fuel consumption with varying equivalence ratio. The figures show that the maximum specific thrust and minimum SFC occur for a stoichiometric mixture, $\emptyset$ = 1.0.

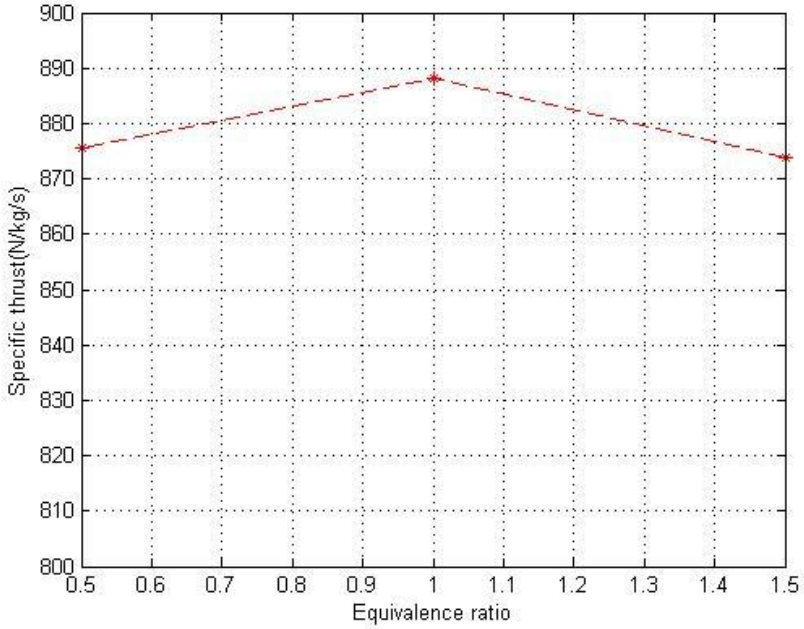

Fig 5.10: Baseline hybrid performance: Specific thrust vs. Equivalence ratio.

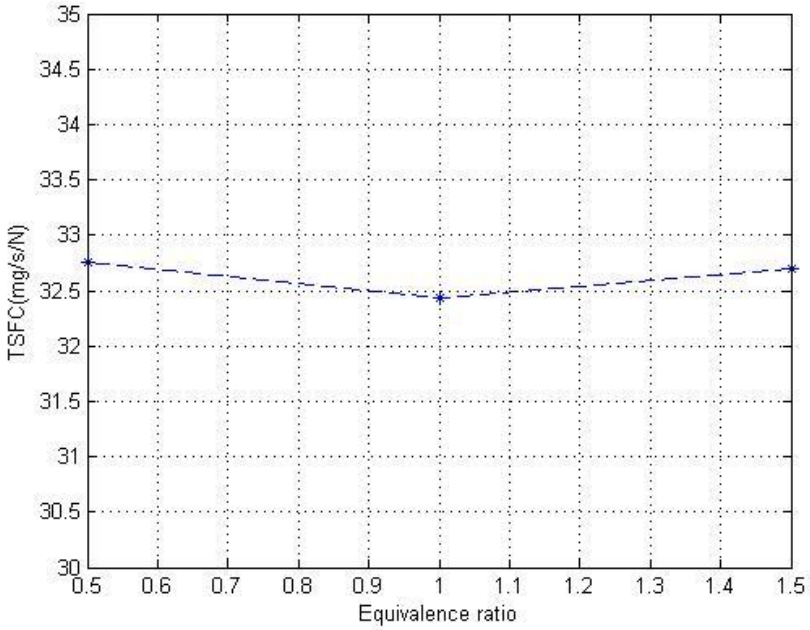

Fig 5.11: Baseline hybrid performance: TSFC vs. Equivalence ratio

Figures 5.12 and 5.13 show the performance of the hybrid PDE/Turbofan engine at sea-level and at an altitude of 45kft. Off design analysis of the baseline hybrid PDE/Turbofan engine at sea-level yielded a gain in specific thrust by 12.9% and balancing that it was an increase of 3.1% in TSFC, and for Mach 2 at an altitude 45000 ft. a gain in specific thrust by 6.2% and an increase in TSFC by 3.9%.

.

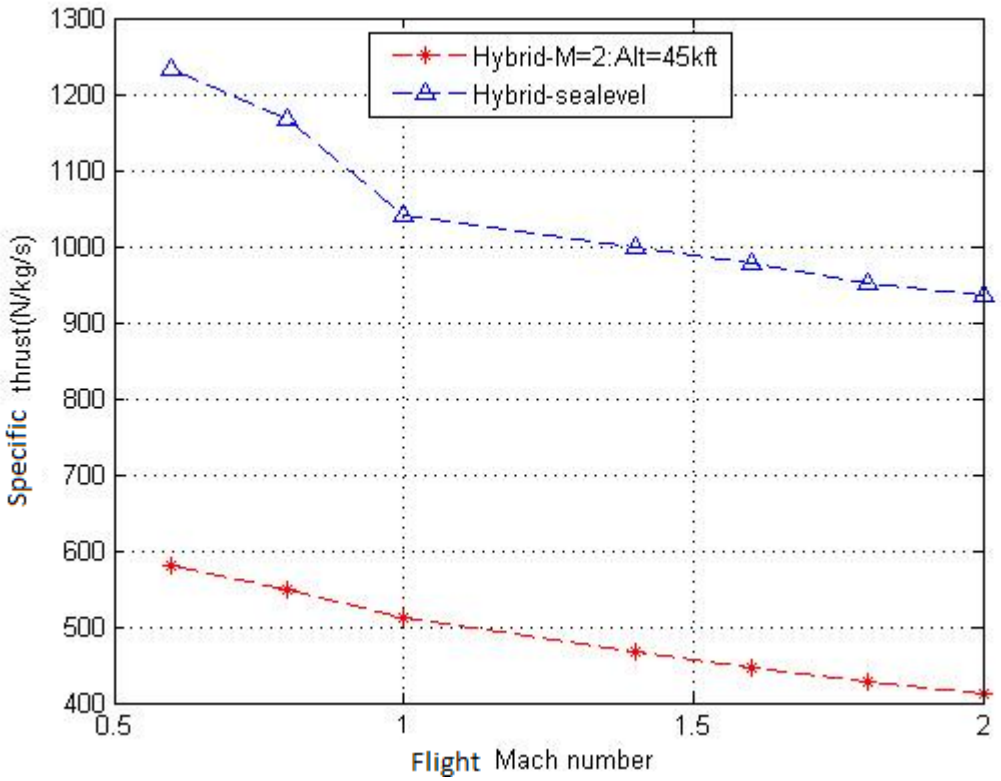

Fig 5.12: Performance of the hybrid engine: Specific thrust at sea level and at altitude 45kft

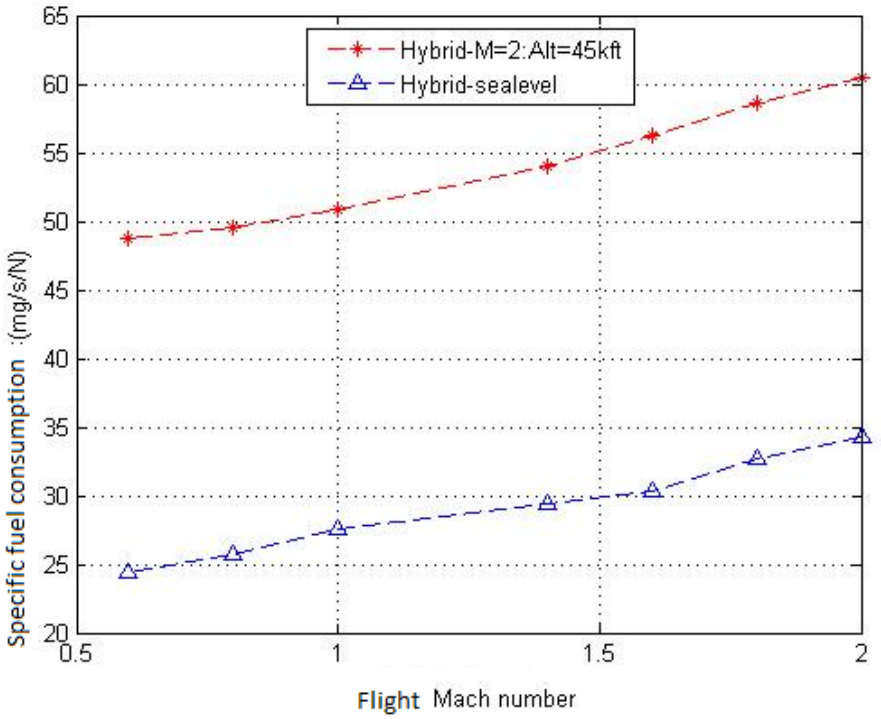

Fig 5.13: Performance of the hybrid engine: TSFC at sea level and at altitude 45kft

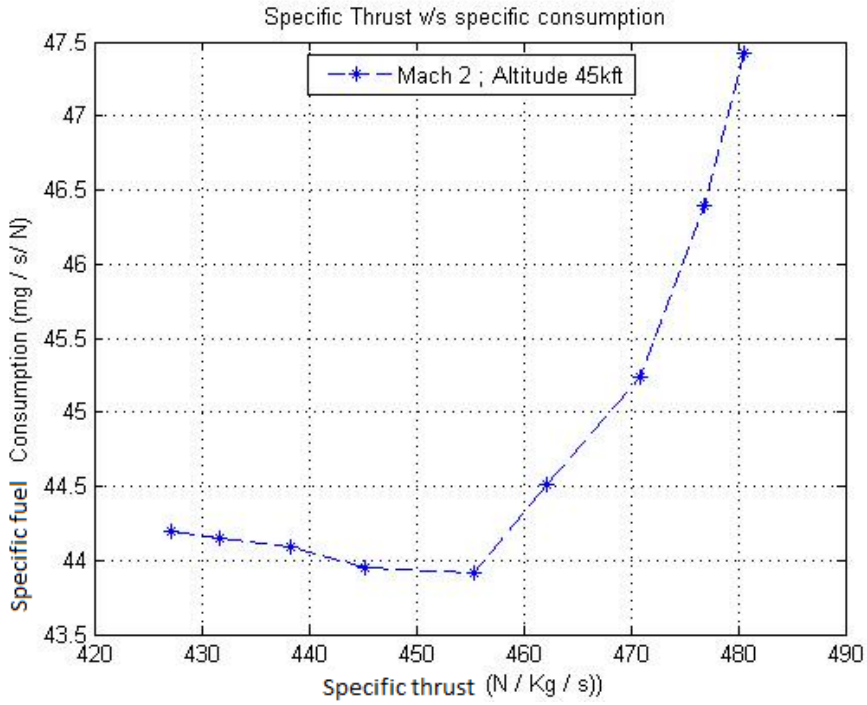

Fig 5.14: Specific fuel consumption vs.specific thrust of hybrid engine at Mach 2 at altitude 45kft

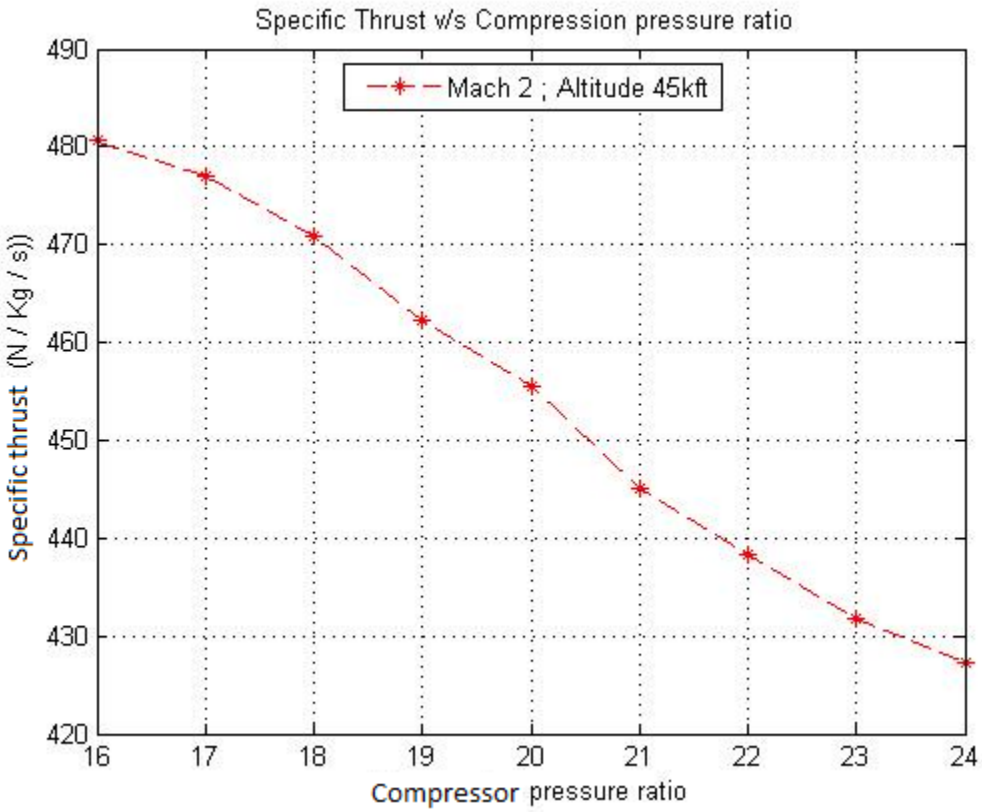

Fig 5.15: Specific thrust of hybrid engine vs. compressor pressure ratio at Mach 2 at altitude 45kft

CHAPTER 6

CONCLUSION AND FUTURE WORK

A parametric and performance cycle analysis of a mixed flow Hybrid Pulse Detonation /Turbofan engine was carried out in this study. A numerical model of the PDE was presented based on an updated model of Endo and Fujiwara [29, 30, and 31]. Effects of different parameters were investigated. Results prove that having PDE combustion chambers in the bypass duct of a turbofan engine boosted the performance, with increase in specific thrust by 11.8% and increased thrust by 7% when compared to the baseline engine. During the mixer analysis the range of Pt16/Pt6 and M16 are limited for mixing to occur without the flow is being choked or having reverse flow. The range of alpha for hybrid engine is 0.8-1. Fan pressure ratio can varied from 3.6- 5.4.Compressor pressure ratio varies from 20-30. The mixer analysis was done The Hybrid PDE code is capable of predicting engine performance by varying altitudes, flight conditions, and frequency of PDE operation, equivalence ratio and length of the tubes.

Recommended work is to perform quasi- steady analysis at each point during PDE cycle to verify that mixer analysis does not breakdown at different points during the PDE cycle.

APPENDIX A

CONSTANT AREA MIXER ANALYSIS

A subsonic constant area mixer with calorically perfect gases is considered for this analysis.

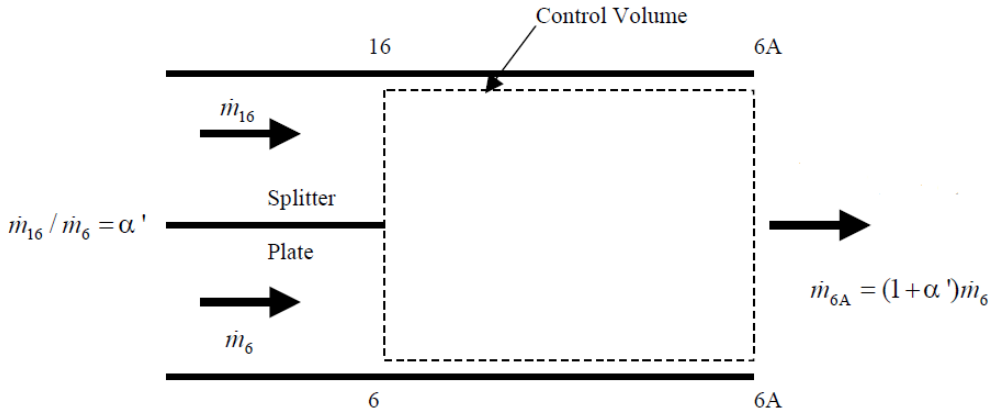

Fig: Constant area mixer.

The gas properties at stations 6 and 16 are given by the following equations

$$\alpha' \doteq \frac{\dot{m}_6}{\dot{m}_{16}} = \frac{\alpha}{(1-\beta-\varepsilon_1-\varepsilon_2)(1+f)+\varepsilon_1+\varepsilon_2} \qquad (1)$$

$$\frac{P_{t16}}{P_{t6}} = \frac{\pi_{PDE}}{\pi_{cL}\pi_{cH}\pi_b\pi_{tH}\pi_{tL}} \qquad (2)$$

$$\frac{T_{t16}}{T_{t6}} = \frac{T_{(avg)}}{T_{t4}\tau_{m1}\tau_{tH}\tau_{m2}\tau_{tL}} \qquad (3)$$

At station at 6A, the properties are given by,

$$c_{p6A} = \frac{c_{p6} + \alpha' c_{p16}}{1+\alpha'}$$
$$R_{6A} = \frac{R_6 + \alpha' R_{16}}{1+\alpha'} \quad (4)$$

The total temperature ratio is given by

$$\tau_M \doteq \frac{T_{t6A}}{T_{t6}} = \frac{c_{p6}}{c_{p6A}} \frac{1+\alpha' \, (c_{p16} T_{t16}) / (c_{p6} T_{t6})}{1+\alpha'} \quad (5)$$

M6A has to has to be found out to find Pi_m because M_6 fixes M_{16}

The pressure ratio is given by

$$\frac{P_{t16}}{P_{t6}} = \frac{\left(1 + \frac{\gamma_{16}-1}{2} M_{16}^2\right)^{\gamma_{16}/(\gamma_{16}-1)}}{\left(1 + \frac{\gamma_6 - 1}{2} M_6^2\right)^{\gamma_6/(\gamma_6-1)}} \quad (6)$$

For the hybrid engine Pt16 is replaced by the average pressure expelled by the PDE tube in the bypass

And M16 is determined by

$$M_{16} = \sqrt{\frac{2}{\gamma_{16}-1}\left\{\left[\frac{P_{t16}}{P_{t6}}\left(1+\frac{\gamma_6-1}{2}M_6^2\right)^{\gamma_6/(\gamma_6-1)}\right]^{(\gamma_{16}-1)/\gamma_{16}}-1\right\}} \quad \textbf{(7)}$$

The area ratio at the mixer entry is given by the following expression

$$\frac{A_{16}}{A_6} = \alpha' \frac{M_6}{M_{16}}\sqrt{\frac{\gamma_6 R_{16}}{\gamma_{16} R_6}\frac{T_{t16}}{T_{t6}}\frac{1+\frac{\gamma_6-1}{2}M_6^2}{1+\frac{\gamma_{16}-1}{2}M_{16}^2}} \quad (8)$$

The Mach number exiting the mixer is given by the following expression

$$M_{6A} = \sqrt{\frac{2\Phi}{(1-2\Phi\gamma_{6A})\mp\sqrt{1-2\Phi(\gamma_{6A}+1)}}} \quad (9)$$

Where,

$$\Phi = \left\{\frac{1+\alpha'}{\frac{1}{\sqrt{\phi(M_6,\gamma_6)}}+\alpha'\sqrt{\frac{R_{16}\gamma_6}{R_6\gamma_{16}}}\sqrt{\frac{T_{t16}/T_{t6}}{\phi(M_{16},\gamma_{16})}}}\right\}^2 \frac{\gamma_6 R_{6A}}{\gamma_{6A} R_6}\tau_M \quad (10)$$

After obtaining the mixer exit Mach number, we can calculate the mixer pressure ratio by the following expression

$$\pi_M = \pi_{Mmax}\ \pi_{Mideal} \qquad (11)$$

Above numerical method is used for obtaining mixer properties and later used for calculating the Specific thrust and specific fuel consumption of the engine.

The parametric analysis of the mixed flow turbofan are carried out by the equations presented by Mattingly's work [35] where bypass ratio (alpha), fan pressure ratio, compressor pressure ratio, and M6 are given as inputs. The performance analysis is similar to the parametric analysis but with incorporating the scaling relationships for the design parameters such as bypass ratio, fan pressure ratio, compressor pressure ratio. The scaling relations are presented below.

$$\tau_{cL} = 1 + \left(\tau_f - 1\right)\frac{\left(\tau_{cL} - 1\right)_R}{\left(\tau_f - 1\right)_R} \tag{11}$$

$$\pi_{cL} = \left\{1 + \eta_{cL}\left(\tau_{cL} - 1\right)\right\}^{\gamma_c/(\gamma_c - 1)} \tag{12}$$

$$\tau_f = 1 + \frac{1 - \tau_{tL}}{(1 - \tau_{tL})_R}\,\frac{\tau_\lambda/\tau_r}{(\tau_\lambda/\tau_r)_R}\,\frac{1 + \alpha_K}{1 + \alpha}\,(\tau_{fR} - 1) \tag{13}$$

$$\pi_f = \left[1 + (\tau_f - 1)\eta_f\right]^{\gamma_c/(\gamma_c - 1)} \tag{14}$$

$$\tau_{cH} = 1 + \frac{T_{t4}/T_0}{(T_{t4}/T_0)_R}\,\frac{(\tau_r\tau_f)_R}{\tau_r\tau_f}\,(\tau_{cH} - 1)_R \tag{15}$$

$$\pi_{cH} = \left[1 + \eta_{cH}(\tau_{cH} - 1)\right]^{\gamma_c/(\gamma_c - 1)} \tag{16}$$

REFERENCES

1. Petters, Dean P. and Felder, James L., “Engine System Performance of Pulse Detonation Concepts Using the NPSS Program". 38th AIAA/AS-ME/SAE/SAE/ASEE Joint Propulsion Conference & Exhibit, AIAA-2002-3910, American Institute of Aeronautics and Astronautics, 2002.

2. Smith, C.F., Snyder, P.H., Emmerson, C.W., and Nalim, M.R., “Impact of the Constant Volume Combustor on a Supersonic Turbofan Engine". 38th AIAA/AS-ME/SAE/SAE/ASEE Joint Propulsion Conference & Exhibit, AIAA-2002-3916. American Institute of Aeronautics and Astronautics, 2002.

4. Heiser, William H. and Pratt, David T., “Thermodynamic Cycle Analysis of Pulse Detonation Engines". AIAA Journal of Propulsion and Power, 2002.

5. Dyer, R.S. and Kaemming, T.A., “The Thermodynamic Basis of Pulsed Detonation Engine Thrust Production". 38th AIAA/ASME/SAE/SAE/ASEE Joint Propulsion Conference & Exhibit, AIAA-2002-4072. American Institute of Aeronautics and Astronautics, 2002.

6. Harris, P.G., Guzik, S.M., and Stowe, R.A., “Design Methodology for a Pulse Detonation Engine as a Ramjet Replacement". 40th AIAA/ASME/SAE/SAE/ASEE Joint Propulsion Conference & Exhibit, AIAA-2004-3400. American Institute of Aeronautics and Astronautics, 2004.

7. Paxson, Daniel E., “A General Numerical Model for Wave Rotor Analysis”, NASA Technical Memorandum NASA-TM-105740, National Air and Space Administration, 1992.

8. Paxson, Daniel E., “A Performance Map for Ideal Air Breathing Pulse Detonation Engines". 37th AIAA/ASME/SAE/ASEE Joint Propulsion Conference &Exhibit, AIAA-2001-3465. American Institute of Aeronautics and Astronautics, 2001.

9. Rasheed, A., Tangirala, V.E., Vandevort, C.L., Dean, A.J., and Haubert, C., “Interactions of a Pulsed Detonation Engine with 2D Blade Cascade". 42nd AIAA Aerospace Sciences Meeting and Exhibit, AIAA-2004-1207. American Institute of Aeronautics and Astronautics, 2004.

10. Tangirala, V.E., Murrow, K., Fakunle, O., and Dean, A.J., “Thermodynamic and Unsteady Flow Considerations in Performance Estimation for Pulse Detonation Applications". 43rd AIAA Aerospace Sciences Meeting and Exhibit, AIAA-2005- 226. American Institute of Aeronautics and Astronautics, 2005.

11. Rasheed, Adam, Furman, Anthony, and Dean, Anthony J., “Wave Attenuation and Interactions in a Pulsed Detonation Combustor-Turbine Hybrid System".44th AIAA Aerospace Sciences Meeting and Exhibit, AIAA-2006-1235. American Institute of Aeronautics and Astronautics, 2006.

12. Rasheed, Adam, Furman, Anthony, and Dean, Anthony J., “Wave Interactions in a Multi-tube Pulsed Detonation Combustor-Turbine Hybrid System". 42nd AIAA/ASME/SAE/ASEE Joint Propulsion Conference & Exhibit, AIAA-2006-4447. American Institute of Aeronautics and Astronautics, 2006.

13. Akbari, P., Nalim, M.R., and Snyder, P.H., “Numerical Simulation and Design of a Combustion Wave Rotor Deflagrative and Detonative Propagation". 42nd /ASME/SAE/ASEE Joint Propulsion Conference & Exhibit, AIAA-2006- 5134. American Institute of Aeronautics and Astronautics, 2006.

14. Nicholas Caldwell, and Ephraim Gutmark*y* “Performance Analysis of a Hybrid Pulse Detonation Combustor / Gas Turbine System” University of Cincinnati , 2005

15. K. Kailasanath.” Review of Propulsion Applications of Detonation Waves engines” AIAA Journal, Vol. 38, No. 9, 2000, pp. 1698–170.

16. Arun Prakash Raghupathy **“**A Numerical Study of Detonation and Plume Dynamics in a Pulsed Detonation Engine”, MS thesis, University of Cincinnati, 2005.

17. Kuo, K.K., “Principles of Combustion,” 2nd Ed., John Wiley and Sons, Inc., 2005.

18. Haider Hekiri., “Parametric Cycle Analysis for Pulse Detonation Engines”, MS Thesis, University of Texas at Arlington, 2005.

19. http://www.pilotbug.com/?tag=engine-technology.

20. K. Kailasanath “Review of Propulsion Applications of Detonation Waves”, Vol. 38, No. 9, September 2000.

21. Nicholls, J. A., Wilkinson, H. R., and Morrison, R. B., “Intermittent Detonation as a Thrust-Producing Mechanism,” Jet Propulsion, Vol. 27, No. 5, 1957, pp. 534–541.

22. Benjamin Zittere., “Flow path design of a three tube valve less pulse detonation”, thesis, Naval post graduate school, September, 2009.

23. http://www.physics.ubc.ca/~lamm/docs/201report.pdf

24.http://www.Airpower.Maxwell.AF.mil/airchronicles/apj/apj04/spr04/kelly.Html

25. Tegner .J, ”Design principles concerning pre detonators in pulse detonation engine” Swedish conference, 1999

26. Mattingly J.D., Heiser W.H., Pratt D.TAircraft engine Design” second edition AIAA series 2002

27. Bussing T and Pappas G.,”Pulse detonation engine theory and concepts”, vol 165 AIAA 1996.

28. Matthew Lam Daniel Tillie, Timothy Leaver, and Brian McFadden., “Pulse Detonation Engine Technology: An overview”, Applied Science 201 the University of British Columbia, 2004.

29. Takuma Endo and Toshi Fujiwara “A Simplified Analysis on a Pulse Detonation Engine Model”, Tans. Japan soc. Aero. Space sci Vol 44, No. 146, pp, 217-222, 2002.

30. Takuma Endo and Toshi Fujiwara., “Analytical Estimation of Performance parameters of an Ideal Pulse Detonation Engine”, Tans. Japan soc. Aero. Space sci Vol 45, No. 150, pp, 249-254, and 2003.

31. Takuma Endo, Jiro kasahara and Toshi Fujiwara., “Pressure history at the thrust wall of a simplified Pulse Detonation Engine” AIAA journal. VOL. 42, NO 9, September 2004.

32. http://www.grc.nasa.gov/WWW/CEAWeb/ceaguiDownload-win.html

33. Mattingly, Jack D "Elements of Gas turbine Propulsion", McGraw-Hill, 2002.

34. Mattingly, Jack D, William H .Heiser, David T Pratt, "Aircraft Engine Design", second edition, 2002.

35. Cumpsty, N., "Jet Propulsion", Cambridge University Press, Cambridge, U.K., 2003. pp 179-262.

36. He, X., and Karagozian, A.R., "Numerical Simulation of Pulse Detonation Engine Phenomena," Journal of Scientific Computing, Vol. 19, Nos. 1-3, December 2003.

37. Kailasanath, K., (2003), "Recent Developments in the Research on Pulse Detonation Engines", AIAA Journal, Vol. 41, No.2, 2003.

38. Kailasanath, K., Patnaik, G., and Li, C., "Computational Studies of Pulse Detonation Engines: 41.A Status Report," AIAA Paper 1999-2634, 35th AIAA/ASME/SAE/ASEE Joint Propulsion Conference and Exhibit, California.

39. Mawid, M. A., Park, T. W., Sekar, B., and Arana, C., "Turbofan Engine Thrust Augmentation with Pulse Detonation Afterburners–Nozzle Influence," AIAA Paper 2002-4073, 38th AIAA/ASME/SAE/ASEE Joint Propulsion Conference and Exhibit, IN.

40. Schauer, F., Bradley, R., and Hoke, J., "Interaction of a Pulsed Detonation Engine with a Turbine," AIAA Paper 2003-0891, 41st Aerospace Sciences Meeting and Exhibit, Reno, NV, 2003..

41. Schauer, F., Stutrud, J., and Bradley, R., "Detonation Initiation Studies and Performance Results for Pulsed Detonation Engine Applications," AIAA Paper 2001-1129, 39th Aerospace Sciences Meeting and Exhibit, Reno, NV.

42. Schultz, E., and Sheperd, J., "Detonation Database: Validation of Detailed Reaction Mechanisms for Detonation Simulation," Explosion Dynamics Laboratory Report FM99-5, Pasadena, CA.

43. Mattingly, Jack D., Heiser, William H., and Pratt, David T., Aircraft Engine Design. American Institute of Aeronautics and Astronautics (AIAA), Reston, Virginia, second edition, 2002**.**

44. Caitlin R. Thorn, Captain, USAF "Off design analysis of a high bypass turbofan using **a** pulse detonation combustor" Air force institute of Technology, Wright-Patterson Air Force Base, Ohio.

45. Andrus, Ionio Q. "Comparative Analysis of a High Bypass Turbofan Using a Pulsed Detonation Combustor".MS thesis, Air force Institute of Technology.

46. Kishore Nekkanti., "Analysis of thrust development in a pulse detonation engine", MS Thesis, University of Texas at Arlington 2010.

47. Louis A. Povinelli ., "Impact of Dissociation and Sensible Heat Release on Pulse Detonation and Gas Turbine Engine Performance" National Aeronautics and Space Administration Glenn Research Center Cleveland, Ohio 44135.

48. http://02b16a8.netsolhost.com/flightinternational.html.

49. Allgood, D. C., "An Experimental and Computational Study of Pulse Detonation Engines," Ph.D. Dissertation, University of Cincinnati, Cincinnati, Ohio 2004.

50.http://www.memagazine.org/backissues/membersonly/nov02/features/plentyrm/plentyrm.htm

51. Carnett, J.B., "How It Works: Pulse Detonation" 2003 Popular Science. 263:3, 53.

52. Rafaela Bellini., "Ideal Cycle Analysis of a Regenerative Pulse Detonation Engine for Power production", Ph.D. Thesis, University of Texas at Arlington 2010.

BIOGRAPHICAL INFORMATION

Sivarai Amith Kumar was born in Akola, Maharashtra, India, in 1987. He received his Bachelor's degree in Aerospace Engineering from Jawaharlal Nehru Technological University, Hyderabad, India, 2008. He joined University of Texas at Arlington to pursue his graduate studies in Aerospace Engineering in the spring 2009. His research interests include Propulsion, Aircraft Structures, CAD Designing, and Numerical models, Gas Dynamics, Hypersonic Combustions and Detonations.